



Published in final edited form as:

Nature. 2018 November ; 563(7731): 402–406. doi:10.1038/s41586-018-0634-9.

A gut microbial factor modulates locomotor behavior in *Drosophila*

Catherine E. Schretter¹, Jost Vielmetter², Imre Bartos³, Zsuzsa Marka³, Szabolcs Marka³, Sulabha Argade⁴, and Sarkis K. Mazmanian¹

¹Division of Biology and Biological Engineering, California Institute of Technology, Pasadena, California

²Protein Expression Center, Beckman Institute, California Institute of Technology, Pasadena, California

³Department of Physics, Columbia University, New York, New York

⁴GlycoAnalytics Core, University of California, San Diego, California

While research into the biology of animal behavior has primarily focused on the central nervous system, cues from peripheral tissues and the environment have been implicated in brain development and function¹. Emerging data suggest bidirectional communication between the gut and the brain affects behaviors including anxiety, cognition, nociception, and social interaction, among others^{1–9}. Coordinated locomotor behavior is critical for the survival and propagation of animals, and is regulated by internal and external sensory inputs^{10,11}. However, little is known regarding influences by the gut microbiome on host locomotion, or the molecular and cellular mechanisms involved. Here we report that germ-free status or antibiotic treatment result in hyperactive locomotor behavior in *Drosophila melanogaster*. Increased walking speed and daily activity found in the absence of a gut microbiome are rescued by mono-colonization with specific bacteria, including the fly commensal *Lactobacillus brevis*. The bacterial enzyme xylose isomerase (Xi) from *L. brevis* is sufficient to recapitulate the locomotor effects of microbial colonization via modulation of sugar metabolism in flies. Notably, we discover that thermogenetic activation of octopaminergic neurons or exogenous administration of octopamine, the invertebrate counterpart of noradrenaline, abrogates Xi-induced effects on *Drosophila* locomotion. These findings reveal a previously unappreciated role for the gut microbiome in modulating

<license-p>Users may view, print, copy, and download text and data-mine the content in such documents, for the purposes of academic research, subject always to the full Conditions of use:<uri xlink:href="http://www.nature.com/authors/editorial_policies/license.html#terms">http://www.nature.com/authors/editorial_policies/license.html#terms</uri></license-p>

Correspondence and requests for materials should be addressed to C.E.S. (cschrett@caltech.edu) or S.K.M. (sarkis@caltech.edu). **Author Contributions** C.E.S. designed, performed, and analyzed most of the experiments. J.V. assisted with experimental design for biochemical analysis. I.B., Z.M., and S.M. assisted with gait analysis experiments. S.A. performed carbohydrate quantification. C.E.S. and S.K.M. supervised the project. C.E.S. and S.K.M. wrote the manuscript with assistance from all of the authors.

Code availability.

Custom code for bout analysis is available from the corresponding authors upon request.

Data availability.

All data sets generated are available from the corresponding authors upon reasonable request.

Author Information The authors declare no competing financial interests.

locomotion, and identify octopaminergic neurons as mediators of peripheral microbial cues that regulate motor behavior in animals.

Coordinated locomotion is required for fundamental activities of life such as foraging, social interaction, and mating, and involves the integration of multiple contextual factors including the internal state of the animal and external sensory stimuli^{10,11}. The intestine represents a major conduit for exposure to environmental signals that influence host physiology, and is connected to the brain through both neuronal and humoral pathways. Recently, seminal studies have uncovered that the intestinal microbiome regulates developmental and functional features of the nervous system^{1,2}, though gut bacterial effects on the neuromodulators and neuronal circuits involved in locomotion remain poorly understood. Since central mechanisms of locomotion, including sensory feedback and neuronal circuits integrating these modalities, are shared in lineages spanning arthropods and vertebrates^{11–13}, we employed the fruit fly *Drosophila melanogaster* to explore host-microbiome interactions that contribute to locomotor behavior. Locomotion was examined in the presence (conventional; Conv) and absence (axenic; Ax) of commensal bacteria. In comparison to conventionally-reared animals, axenic female adult flies exhibit increased walking speed and daily activity (Fig. 1a – b, and 1g). *Drosophila* locomotion is characterized by a pattern of intermittent periods of pauses and activity bouts^{11,14}, during the latter of which the average speed of the fly is above a set threshold of 0.25 mm/second. An increased average speed may be related to changes in temporal patterns, including the number and/or duration of walking bouts¹⁴. We discovered that axenic flies display an increased average walking bout length in addition to a decreased average pause length, while remaining indistinguishable in the number of bouts compared to animals harboring a microbial community (Fig. 1c – f). These data reveal that the microbiota modulates walking speed and temporal patterns of locomotion in *Drosophila*.

The microbial community of *Drosophila melanogaster* contains 5 – 20 bacterial species^{15,16}. In laboratory-raised flies, two of the dominant species are *Lactobacillus brevis* and *Lactobacillus plantarum*¹⁵. Specific bacteria in this community affect distinct features of *Drosophila* physiology, and even closely related microbial taxa can exhibit unique biological influences on the host^{15,17,18}. Accordingly, we examined whether locomotor performance was impacted differentially by individual bacterial species. Despite similar levels of colonization (Extended Data Fig. 1a), mono-association with *L. brevis*, but not *L. plantarum*, starting at eclosion is sufficient to correct speed and daily activity deficits in axenic flies (Fig. 1a– b, 1g, and Extended Data Fig. 1b – e). Varying the strain of *L. brevis* or host diet did not alter bacterial influences on host speed (Extended Data Fig. 1c – e), and *L. brevis* is able to largely restore temporal patterns of locomotion (Fig. 1c – f and Extended Data Fig. 1f). Detailed gait analysis reveals that *L. brevis*-associated flies display comparable locomotor coordination to that of conventionally-reared flies (Fig. 1h and Extended Data Fig. 1g). Further, axenic flies co-colonized with a 1:1 mixture of *L. brevis* and *L. plantarum* display similar changes in speed to flies mono-associated with *L. brevis* (Extended Data Fig. 1h).

To investigate whether the effects of microbial exposure are dependent on host developmental stage, we mono-colonized flies at 3 – 5 days post-eclosion (Extended Data

Fig. 2a), a time point in which the development of the GI tract and remodeling of the nervous system are complete^{19–21}. Colonization with *L. brevis* in fully developed animals decreases locomotor speed and average walking bout length to levels similar in flies treated immediately following eclosion (Extended Data Fig. 2b – e). Changes in locomotion are likely independent of bacterial effects on host development, as conventionally-reared flies treated after eclosion with broad spectrum antibiotics exhibit similar walking speeds to animals born under axenic conditions (Extended Data Fig. 2f). Administration of antibiotics increases fly locomotion in two different wild-type lines (Extended Data Fig. 2g). Furthermore, colonization with *L. brevis*, but not *L. plantarum*, after the removal of antibiotics reduces locomotor behavior to levels similar to conventional flies (Fig. 1i and Extended Data Fig. 2h – l). From these data, we conclude that locomotion is modulated by select bacterial species of the *Drosophila* microbiome, and is mediated by active signaling, rather than developmental influences.

Gut bacteria secrete molecular products that regulate aspects of host physiology, including immunity and feeding behavior^{22,23}. To explore how microbes influence locomotion, we administered either cell-free supernatant (CFS) harvested from bacterial cultures or heat-killed bacteria to axenic flies. CFS alone from *L. brevis* (*L.b* CFS) reduces hyperactivity in axenic flies, while heat-killing bacteria ablates modulation of locomotion (Fig. 2a and Extended Data Fig. 3a – e), demonstrating a requirement for metabolically active *L. brevis*. Previous studies have revealed that *L. brevis* produces uracil¹⁸, a molecule that affects the host immune response and may impact locomotion²². However, administration of physiologic levels of uracil to axenic flies did not alter walking speed (Extended Data Fig. 3f). We next explored whether immunity or feeding behavior impact microbial-mediated locomotion. Depletion of the microbiome in Immune Deficiency (IMD) and Toll knockout flies using antibiotics results in similar increases in walking speed compared to wild-type flies (Extended Data Fig. 4a – b). There are no differences in the expression of anti-microbial peptides or the dual oxidase gene, *Duox*, in *L.b* CFS-treated axenic flies (Extended Data Fig. 4c). Moreover, while food intake may be influenced by bacterial species and can inhibit locomotor behavior^{23–25}, there is no significant change in the amount of food ingested by *L.b* CFS-treated flies compared to controls (Extended Data Fig. 4d – e).

Bacterial metabolism of amino acids and carbohydrates is associated with changes in host behavior^{6,8}; however, it is not known whether bacterial metabolic enzymes influence host locomotion. Employing biochemical analysis of *L.b* CFS and comparative functional analysis of bacterial strains^{26–28}, we determined that bacterial locomotor effects are mediated via proteinaceous molecule(s) present in select bacteria, including *L. brevis* and *E. coli* (Extended Data Fig. 5a – e). Subsequently, a screen of *E. coli* strains containing single gene mutations related to amino acid and carbohydrate metabolism identified xylose isomerase (Xi) as a candidate factor modulating locomotor behavior (Extended Data Fig. 5f). Xi is an enzyme that catalyzes the reversible isomerization of certain sugars, including the conversion of D-glucose to D-fructose²⁹, and is present only in *L. brevis* and *E. coli* of the bacterial strains tested (Extended Data Fig. 5e). Administration of His-tagged Xi from *L. brevis* (Xi*) reduces locomotor behavior in axenic flies to levels similar to *L.b* CFS and conventional flies (Fig. 2b – c and Extended Data Fig. 5g – h). The addition of His-tagged L-arabinose isomerase (Ai*), an enzyme that is not differentially expressed among the

bacteria tested, is not sufficient to influence host speed in axenic flies (Fig. 2c). Furthermore, we generated a chromosomal deletion of the xylose isomerase gene *xyIA* in *L. brevis*, and demonstrate the mutant strain lacks the ability to modulate host speed and daily activity (Fig. 2d and Extended Data Fig. 5g). No changes in survival or intestinal cellular apoptosis occur at the time of motor testing (Extended Data Fig. 5i – j). Additionally, Xi*-treatment did not significantly alter sleep in axenic flies (Extended Data Fig. 6). Neither the addition of predicted products of Xi (D-fructose, D-glucose, D-xylose, and D-xylulose) alone, nor Xi inactivated by EDTA treatment²⁹, reduces walking speed in axenic flies (Extended Data Fig. 7a – c). We next sought to explore Xi activity through carbohydrate analysis of whole flies, which revealed flies given Xi* exhibit increased ribose and reduced trehalose levels compared to axenic controls (Fig. 2e), with no differences in these sugars in the fly media (Extended Data Fig. 7d). While EDTA-treated Xi* did not significantly alter trehalose levels, these flies still display heightened levels of ribose compared to axenic controls (Extended Data Fig. 7e). Additionally, similar to previous findings³⁰, conventional and *L. brevis*-colonized flies show reduced levels of trehalose compared to axenic groups (Extended Data Figures 7f – g). Administration of trehalose alone reverses microbial effects on host speed, while supplementation with arabinose or ribose does not (Fig. 2f and Extended Data Fig. 7h – k). Collectively, these results demonstrate that xylose isomerase from *L. brevis* is sufficient to control locomotion in *Drosophila*, likely via modulation of key carbohydrates, such as trehalose.

Specific neuronal pathways regulate complex behaviors in animals^{31–33}, and can be modulated by peripheral inputs, including intestinal and circulating carbohydrate levels³⁴. To explore the involvement of various neuronal subsets in bacterial-induced motor behavior, we used the thermosensitive cation channel *Drosophila* TRPA1 (dTRPA1) to activate neuronal populations previously implicated in locomotion³⁵, via a repertoire of GAL4-driver lines. In combination with *UAS-dTipA1* at the activity-inducing temperature (27°C), we observe that activation of only two GAL4 lines that both label octopaminergic neurons, tyrosine decarboxylase (*Tdc2*) and tyramine beta-hydroxylase (*Tβh*), override *L. brevis* modulation of locomotion (Fig. 3a and Extended Data Fig. 8). Accordingly, activation of *Tdc*-expressing cells abrogated the effects of Xi*-treatment and differences between conventional and antibiotic-treated groups (Fig. 3b – c and Extended Data Fig. 9). The ability of *L. brevis* to decrease locomotion, however, is not changed by the activation of dopaminergic, serotonergic, GABAergic, or cholinergic neurons (Fig 3a and Extended Data Fig. 8e – h). The administration of octopamine to conventional, Xi*-, or *L.b* CFS-treated flies increases host walking speed to levels similar to that of axenic flies (Fig. 3d – e and Extended Data Fig. 10a). Further, *Tdc2* and *Tβh* transcript levels are reduced in RNA extracted from the heads of Xi*- and *L.b* CFS-treated flies (Extended Data Figure 10b – c). As *Tdc* and *Tβh* are important for octopamine synthesis, these results further link octopamine to Xi-induced locomotor effects. Octopamine and tyramine are involved in multiple aspects of host physiology, including metabolism and behavior, and display opposite roles in regulating certain motor behaviors^{36–44}. While administration of tyramine did not influence walking speed in Xi* and *L.b* CFS conditions (Fig. 3e and Extended Data Fig. 10d), antibiotic-treated flies carrying a null allele for *Tdc* (*Tdc2^{RO54}*) no longer display differences in locomotion upon supplementation with Xi* (Fig. 3f), suggesting an indirect

role for tyramine. Limiting the expression of a transgene for diphtheria toxin (*DTI*) to octopaminergic and tyramineric neurons outside of the ventral nerve cord^{39,45} results in equivalent average speeds between antibiotic and Xi*-treated flies (Extended Data Fig. 10e), implicating the involvement of neurons in the supraesophageal and the subesophageal zones in microbial effects on motor behavior. Octopamine signaling is necessary for locomotor changes, as axenic flies administered with mianserin, an octopamine receptor antagonist, and antibiotic-treated flies carrying a null allele for T β h (*T β H^{M18}*) or expressing T β h RNAi no longer respond to Xi* or *L.b* CFS treatment (Fig. 3g and Extended Data Fig. 10f – h). Similar results are also found under conventional conditions compared to antibiotic-treated groups (Extended Data Fig. 10i – k). Collectively, we conclude that defined products of the microbiome, and specifically Xi, negatively regulate octopaminergic pathways to control *Drosophila* locomotion (Extended Data Fig. 10l).

The microbiome influences neurodevelopment, regulates behavior, and contributes to various neurologic and neuropsychiatric disorders. Herein, we demonstrate that gut bacteria modulate locomotion in female *Drosophila*. The depletion of the gut microbiota increases host exploratory behavior, and the commensal bacterium *L. brevis* is sufficient to regulate locomotion. In addition, we establish that xylose isomerase from *L. brevis* corrects the locomotor phenotypes of axenic flies, a process that is mediated by trehalose and octopamine signaling in the host. However, further work is needed to identify the exact neurons and neuronal mechanisms involved, including potential changes in firing patterns. It would also be important to clarify the sex-specific aspects of these microbial effects on locomotion^{30,46}. It is intriguing that germ-free mice display hyperactivity similar to axenic *Drosophila*, and specific bacteria have been shown to decrease locomotor activity in mice^{1,47,48}, although the neuronal pathways implicated in mammalian systems have yet to be identified. The mammalian counterpart of octopamine, noradrenaline, modulates locomotion^{31,49}, potentially implicating adrenergic circuitry as a conserved pathway that is co-opted by the microbiome in flies and mammals. In addition to motor behavior, octopamine signaling is linked to sugar metabolism, and trehalose serves as a major energy source for *Drosophila*³⁶. Xylose isomerase may therefore facilitate adrenergic regulation of host physiology through orchestrating metabolic homeostasis, such as via altering internal energy storage, although additional work is needed to define how the microbiome mediates interactions between sugar metabolism and octopamine signaling. The inextricable link between metabolic state and locomotion suggests that peripheral influences on metabolism may signal via neuronal pathways to modulate physical activity. As animals have become metabolically intertwined with their microbiomes, perhaps it is not surprising that a fundamental trait such as locomotion is influenced by host-microbial symbiosis.

METHODS

Fly Stocks and Rearing.

We obtained Canton-S (#64349), *Imd*^{-/-} (#55711), *Ti*^{-/-} (#30652), *UAS-dTrpA1* (#26264), *Tdc2-GAL4* (#52243), *T β h-GAL4* (#48332), *Th-GAL4* (#8488), *Ddc-GAL4* (#7009), *Gad1-GAL4* (#51630), *ChAT-GAL4* (#60317), *Elav-GAL4* (#46655), *UAS-T β h^{RNAi}* (#27667), *UAS-DTI* (#25039), and *pBDPG4U-GAL4* (#68384) lines from Bloomington

Drosophila Stock Center at Indiana University. Other fly stocks used were Oregon^R (kindly provided by A. A. Aravin and K. Fejes Tóth), *TβH^{M18}* (kindly provided by M. H. Dickinson)⁵⁰, *Tdc2^{R054}*, and *tsh-GAL80* (both kindly provided by D. J. Anderson)^{51,52}. To minimize the effect of genetic background on behaviors, mutant fly lines were outcrossed for at least three generations onto a wild-type background.

Flies were cultured at 25°C and 60% humidity on a 12-hr. light:12-hr. dark cycle and kept in vials containing fresh fly media made at California Institute of Technology consisting of cornmeal, yeast, molasses, agar, p-hydroxy-benzoic acid methyl ester. Other dietary compositions used were created through altering this standard diet or the Nutri-Fly “German Food” Formula (Genesee Scientific) and were calculated using previously published nutritional data⁵³. Axenic flies were generated using standard methods^{18,54–58}. Briefly, embryos from conventional flies were washed in bleach, ethanol, and sterile PBS before being cultivated on fresh irradiated media⁵⁴. Axenic stocks were maintained through the application of an irradiated diet supplemented with antibiotics (500 µg/ml ampicillin, Putney; 50 µg/ml tetracycline, Sigma; 200 µg/ml rifamycin, Sigma) for at least one generation. For experiments, virgin female flies were collected shortly after eclosion and placed at random into vials (10 – 15 flies per vial) containing irradiated media without antibiotics. Vials were changed every 3 – 4 days using sterile methods. The antibiotic supplemented diet was applied to conventional flies shortly after eclosion to generate antibiotic-treated (ABX) flies. Both antibiotic-treated and axenic flies were tested for contaminants through plating animal lysates on Man, Rogosa, and Sharpe (MRS, BD Biosciences), Mannitol (25 g/L Mannitol, Sigma; 5 g/L Yeast extract, BD Biosciences; 3 g/L Peptone, BD Biosciences), and Luria-Bertani (LB, BD Biosciences) nutrient agar plates.

Bacterial Strains.

Lactobacillus brevis^{EW}, *Lactobacillus plantarum*^{WJL}, and *Acetobacter pomorum* were obtained from laboratory-reared flies in the laboratory of Won-Jae Lee (Seoul National University)^{18,56,58}. *Lactobacillus brevis*^{Bb14} (ATCC, #14869) and *Lactobacillus brevis*^{P-2} (ATCC, #27305) were isolated from human feces and fermented beverages, respectively. *Escherichia coli*^{K12} (CGSC, #7636) was grown in LB broth and *Escherichia coli*^{tyrA} (CGSC, #9131), *Escherichia coli*^{trpC} (CGSC, #10049), *Escherichia coli*^{manX} (CGSC, #9511), *Escherichia coli*^{treA} (CGSC, #9090), and *Escherichia coli*^{xyIA} (CGSC, #10610)²⁸ were grown in LB broth supplemented with kanamycin (50 µg/mL). *Lactobacillus brevis* and *Lactobacillus plantarum* cultures were grown overnight in a standing 37°C incubator in MRS broth (BD Biosciences). For mono-associations, fresh stationary phase bacterial cultures (OD₆₀₀ = 1.0, 40 µL) were added directly to fly vials. Associations with two bacteria were performed in a 1:1 mixture. For heat-killed experiments, fresh cultures of *Lactobacillus brevis* (OD₆₀₀ = 1.0) were washed 3 times in sterile PBS, incubated at 100°C for 30 min., and cooled to room temperature before administering to flies. All treatments were supplied daily through application to the fly media (40 µL) for 6 days following eclosion.

Bacterial Supernatant Preparations.

Cell-free supernatants (CFS) of specified bacterial strains were harvested from bacterial cultures ($OD_{600} = 1.0$) by centrifuging at $13,000 \times g$ for 10 min. and subsequent filtration through a 0.22- μm sterile filter (Millipore). CFS was dialyzed in MilliQ water with a 3.5 kDa membrane (Thermo Scientific) overnight at 4°C to generate *L.b* CFS and *L.p* CFS samples. Each of these treatments were supplied daily through application to the fly media (40 μL) for 6 days following eclosion.

Heat and Enzymatic Treatment of *L.b* CFS.

For heat-inactivation experiments, freshly prepared *L.b* CFS samples were incubated at 100°C for 30 min. and cooled to room temperature before administering to flies. For proteinase K (PK) and trypsin (Typ) treatment, overnight dialysis of CFS was performed in Tris-HCl (pH 8 for PK and pH 8.5 for Typ) after which samples were treated with either PK (100 $\mu\text{g}/\text{mL}$, Invitrogen) or Typ (0.05 $\mu\text{g}/\text{mL}$, Sigma) at 37°C for 24 or 7 hrs., respectively. A proteinase inhibitor cocktail (Sigma) was added to stop the reaction and subsequently removed through overnight dialysis (Thermo Scientific) at 4°C in MilliQ water. Aliquots of the samples were run on a 4–20% Tris-glycine gel (Invitrogen) to confirm protein cleavage. Controls followed the same protocol except for the addition of proteinase K or trypsin. For amylase digests, 20 μL of 100 mU/mL amylase (Sigma) was added to either freshly prepared *L.b* CFS or a PBS control for 30 min. and inhibited through lowering the pH to 4.5. Each of these treatments were supplied daily through application to the fly media (40 μL) for 6 days following eclosion.

Production of His-tagged proteins (Xi* and Ai*)

An expression plasmid for the production of His-tagged xylose isomerase from *L.b*, here termed as Xi*, was constructed by amplification of its gene and cloning the resulting PCR product in the pQE30 cloning vector (Qiagen) using SLIC ligation. The following primer sequences were used for the construct: 5'-CGCATCACCATCACCATCACGGATCTTACTTGCTCAACGTATCGATGATGTAA-3' and 5'-GGGGTACCGAGCTCGCATGCGGATCATGACTGAAGAATACTGGAAAGGC-3'. Conformation of the resulting plasmid was verified and transformed into *E. coli* (Turbo, NEB). This strain was then grown in LB containing ampicillin (100 $\mu\text{g}/\text{mL}$) and chloramphenicol (25 $\mu\text{g}/\text{mL}$) with shaking at 220 rpm at 37°C for 1 hr. before the addition of 0.1 mM IPTG. After 4 hrs. of shaking at 220 rpm at 37°C, cells were pelleted and lysed using lysozyme (Sigma) and bead beating with matrix B beads (MP Biomedicals) for 45 sec. Supernatant was collected after centrifugation and the Xi* protein purified through metal affinity purification under native conditions using HisPur™ Ni-NTA Spin Columns (Thermo Scientific). Protein purification was verified through western blot using an Anti-6X His tag® antibody (Abcam) and quantified using a Pierce BCA Protein Assay kit (Thermo Scientific) after which protein was stored at –20°C. Expression and purification of His-tagged L-arabinose isomerase from *L.b*, here termed as Ai*, was performed under the exact same conditions and the following primer sequences were used for the construct: 5'-GGGGTACCGAGCTCGCATGCGGATCATGTTATCAGTTCCAGATTATGAATTTTGG-3

' and 5'-

CGCATCACCATCACCATCACGGATCCTTACTTGATGAACGCCTTTGTCAT-3'. For EDTA treatment²⁹, purified Xi* was combined with 5 mM EDTA for 44 hrs. at 4°C and subsequently dialyzed prior to administering to flies through application to the fly media (40 µL) for 6 days following eclosion.

Generation of *xyIA* deletion mutant (*xyIA*)

~1-kb DNA segments flanking the region to be deleted were PCR amplified using the following primers: 5'-ATTCCAATACTACCACTAGCAACGACATCCGTAAGT-3'; 5'-AATTCGAGCTCGGTACCCGGGATCCACAATCAGAATTGATCGCGGCAAC-3'; 5'-TCGTTGCTAGTGGTAGTATTGGAATCCTAAACCAGATTTCTTATCTTGATG-3'; 5'-GCCTGCAGGTCGACTCTAGAGGATCCCGCAAGTCTAGTGCGGCT-3'. The forward primers were designed using to be partially complementary at their 5' ends by 25 bp. The fused PCR product was cloned into the BamHI site of the *Lactobacilli* vector pGID023 and mobilized into *L.b.* Colonies selected for the erythromycin (Erm) resistance, indicating integration of the vector into the host chromosome were re-plated onto MRS+Erm and subsequently passaged over 5 days and plated onto MRS+Erm. Colonies selected for Erm resistance were passaged again in MRS alone over 3 days and plated on MRS. Resulting colonies were plated in replica on MRS and MRS+Erm. Erm sensitive colonies were screened by PCR to distinguish wild-type revertants from strains with the desired mutation.

Drug treatments.

Axenic flies were either left untreated or administered with *L.b* CFS or Xi* for 3 days after eclosion. After switching to new irradiated fly media, groups of axenic flies were treated through application to the fly media (40 µL) with octopamine (OA, 10 mg/mL, Sigma), tyramine (TA, 10 mg/mL, Sigma), L-dopa (1 mg/mL, Sigma), or mianserin (2 mg/mL) every day for 3 days before testing, similar to previously published methods^{33,37}.

Bacterial Load Quantification.

Intestines dissected from surface sterilized 7-day-old adult female flies were homogenized in sterile PBS with ~100 µl matrix D beads using a bead beater. Lysate dilutions in PBS were plated on MRS agar plates and enumerated after 24 hrs. at 37°C.

Locomotion Assays.

Locomotor behavior was assayed through three previously established methods: the *Drosophila* Activity Monitoring System (DAMS, Trikinetics)^{59,60}, video-assisted tracking^{61–63}, and gait analysis⁶⁴.

Activity measurements.—7-day-old individual female flies were cooled on ice for 1 min. and transferred into individual vials (25 × 95 mm) containing standard irradiated media. Tubes were then inserted and secured into *Drosophila* activity monitors (DAMS, Trikinetics) and kept in a fly incubator held at 25°C. Flies were allowed to acclimate to the new environment for 1 day before testing and midline crossing was sampled every min. Average daily activity was calculated from the 2 days tested and actograms were generated

using ActogramJ⁶⁰. Sleep was defined as a 5 min. bout of inactivity as previously described⁶⁵.

Video-assisted tracking.—Individual female flies were cooled on ice for 1 min. before being introduced under sterile conditions into autoclaved arenas (3.5 cm diameter wells), which allowed free movement but restricted flight. After a 1 hr. acclimation period, arenas were placed onto a light box and recorded from above for a period of 10 min. at 30 frames per sec. All testing took place between ZT 0 and ZT 3 (ZT, Zeitgeber time; lights are turned on at ZT 0 and turned off at ZT 12) and both acclimation and testing occurred at 25°C unless otherwise stated. Videos were processed using Ethovision software or the Caltech FlyTracker (<http://www.vision.caltech.edu/Tools/FlyTracker/>).

Bout analysis was performed using custom python scripts (available upon request). The velocity curve was smoothed from the acquired video at 30 frames per sec. using a 15 sec. moving average window. A minimum walking speed of 0.25 mm/s was given below which flies were moving but not walking ('pause bouts') and above which they were designated as walking ('walking bouts'). Lengths were measured as time between bout onset and offset.

Gait analysis.—Experiments used an internally illuminated glass surface with frustrated total internal reflection (FTIR) to mark the flies' contact with the glass⁶⁴. The movement of the flies and their contact was recorded with a high-framerate camera, and videos were quantified using the FlyWalker software package. For further details of the parameters see ⁶⁴. All groups consisted of 7-day-old female flies and were tested at room temperature.

Feeding Assays.

Female flies were collected at the same time as described for *Locomotor Assays*. Flies were transferred regularly onto fresh food until day 7, upon which the flies were starved for 2 hrs. and subsequently transferred for 30 min. to an irradiated standard fly media dyed with FD&C Blue no. 1 (Sigma) at a final concentration of 0.5 g dye per 100 g food. Flies were allowed to feed on the food (3–4 biological replicates and 7 flies per replicate) at 25°C after which they were decapitated and their bodies collected. Each replicate was homogenized in 150 µL of PBS/0.05% Triton X-100 and centrifuged at 5,000 × *g* for 1 min. to remove debris. Absorbance for all groups was measured together at 630 nm and the amount of food consumed was estimated from a standard curve of the same dye solution. The MAFE assay was performed as described previously^{66–67}. Briefly, individual flies were introduced into a 200 µL pipette tip, which was cut to expose the proboscis. Flies were first water satiated and presented with 100 mM sucrose delivered in a fine graduated capillary (VWR). After flies were unresponsive to 10 food stimuli, the assay was terminated and the total volume of food was calculated.

Measurement of life span

Adult female flies were transferred under sterile conditions to irradiated fly media every 4 – 5 days. Survival in 3 or more independent cohorts containing 15 – 25 flies each was monitored over time.

Apoptosis assay

Midguts from 7-day-old female flies were dissected in PBS containing 0.1% Triton X-100 and the apoptosis assay was performed as previously described^{18,56}. The percentage of apoptotic cells was determined by dividing the number of apoptotic cells by the total number of cells in each section and multiplying by 100.

Measurement of carbohydrate levels

Fly (5 flies per sample) and fly media (0.1 g per sample) were homogenized in TE Buffer (10 mM Tris, pH = 8, 1 mM EDTA) using a bead beater for 45 sec. followed by centrifugation at $7,000 \times g$ for 3 min. The supernatant was heat treated for 30 min. at 72°C before being stored at -80°C before subsequent clean-up steps prior to running on HPAEC-PAD.

100 μ L of fly or fly media homogenate sample in TE buffer was diluted with 200 μ L of UltraPure distilled water (Invitrogen) and sonicated to get uniform solution. Samples were centrifuged at 2,000 rpm for 15 sec. to precipitate insoluble material. 100 μ L of the sample was filtered through pre-washed Pall Nanosep® 3K Omega centrifugal device (MWCO 3KDa, Sigma-Aldrich) for 15 min. at 14,000 rpm, 7°C. The filtrate was dried on Speed Vac. The dry sample was reconstituted in 300 μ L of UltraPure water and loaded onto pre-washed Dionex OnGuard® IHH 1cc cartridge. The flow through and 2 \times 1 mL elution with Ultrapure water was collected in the same tube and lyophilized.

Monosaccharide analysis was done using Dionex CarboPac™ PA1 column (4X250mm) with PA1 guard column (4 \times 50mm). Flow rate 1ml/min. Pulsed amperometric detection with gold electrode. The elution gradient was as follows: 0 min. – 20 min., 19 mM sodium hydroxide; 20 min. – 50 min., 0 mM - 212.5 mM sodium acetate gradient with 19 mM sodium hydroxide; 50 min. – 65 min., 212.5 mM sodium acetate with 19 mM sodium hydroxide; 65 min. – 68 min., 212.5 mM – 0 mM sodium acetate with 19 mM sodium hydroxide; 68 min. – 85 min., 19 mM sodium hydroxide

Trehalose, arabinose, galactose, glucose, mannose, xylose, fructose, ribose, sucrose and xylulose were used as standards. The monosaccharides were assigned based on the retention time and quantified using Chromeleon™ 6.8 chromatography data system software. In Extended Data Figures 7f – g, measurements of trehalose levels were performed following the same isolation procedure and subsequently processed using a Trehalose Assay Kit (Megazyme) according to the manufacturer's instructions.

For experiments treating flies with trehalose, arabinose, or ribose, groups of axenic or axenic flies previously treated with Xi* were administered with trehalose, arabinose, or ribose (10 mg/mL, Sigma) through application to the fly media (40 μ L) for every day for 3 days before testing.

RNA isolation and quantitative real-time PCR.

Heads (20 flies per sample) or decapitated bodies (5 flies per sample) were dissected on ice and immediately processed using an Arcturus™ PicoPure™ RNA isolation kit (Applied Biosystems) or a standard TRIzol™-Chloroform protocol (ThermoFisher). 1 μ g of RNA was

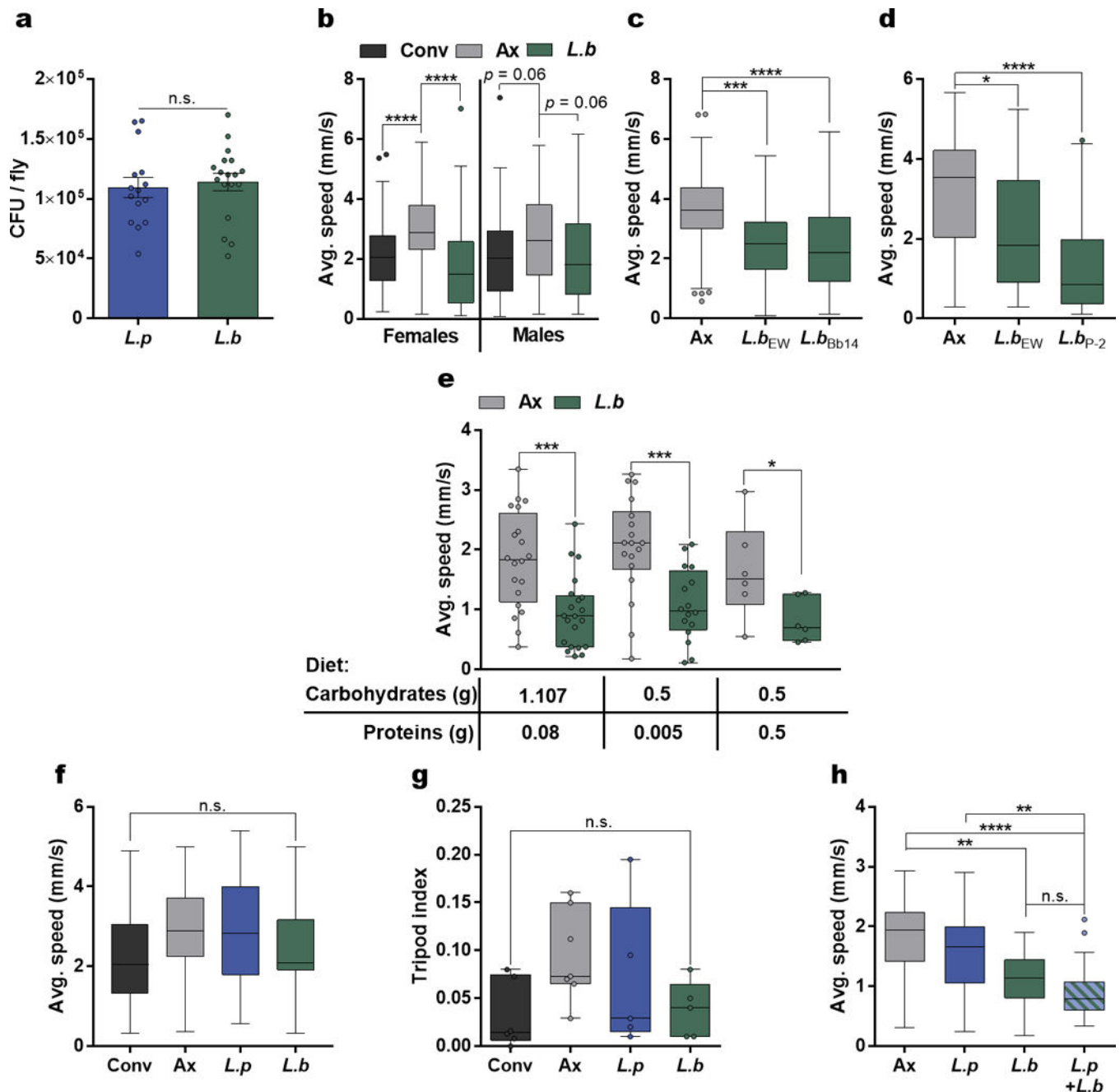
reverse transcribed using iScript cDNA Synthesis Kit, according to manufacturer's protocol (Bio-Rad) and diluted to 10 ng/ μ L based on the input concentration of total RNA.

Previously published primer pairs were used to target immune-related gene transcripts^{18,68}. Other primer sequences used include *Tdc* (F: GGTCTGCCGGACCACTTTC, R: CACTCCGATGCGGAAGTCTG), *T β h* (F: GCTTATCCGACACAAAGCTGC, R: GAAAGCATTCTGCAAGTGGAA), *Ddc* (F: TGGGATGAGCACACCATCTTG, R: GTAGAAGGGAATCAAACCCTCG), *Tph* (F: TGTTTTCGCCCAAGGATTCGT, R: CACCAGTTTATGTCATGCTTCT). All primers were synthesized by Integrated DNA Technologies. Real-time PCR for the house-keeping genes Rp49 and RpL32 were used to ensure that input RNA was equal among all samples. Real-time PCR was performed on cDNA using an ABI PRISM 7900 HT system (ThermoFisher) according to the manufacturer's instructions.

Data reporting and statistical analysis.

Sample size was based on previous literature in the field and experimenters were not blinded as almost all data acquisition and analysis was automated. After eclosion, virgin female flies with the same genotype were sorted into groups of 10–15 flies per vial at random. All flies in each vial were administered with the same treatment regime. For each experiment, the experimental and control flies were collected, treated, and tested at the same time. A Mann-Whitney *U* or Kruskal-Wallis and Dunn's post-hoc test was used for statistical analysis of behavioral data and carbohydrate analysis. Comparisons with more than one variant were first analyzed using Two-way ANOVA. An unpaired two-sided Student's *t*-test or a One-way ANOVA followed by a Bonferroni post-hoc test was used for statistical analysis of quantitative RT-PCR results and CFU analysis. All statistical analysis was performed using Prism Software (GraphPad, version 7). *P* values are indicated as follows: **** $P < 0.0001$; *** $P < 0.001$; ** $P < 0.01$; and * $P < 0.05$. See Supplementary Material for more details on statistical tests and exact *P* values for each figure. For boxplots, lower and upper whiskers represent 1.5 interquartile range of the lower and upper quartiles, respectively; boxes indicate lower quartile, median, and upper quartile, from bottom to top. When all points are shown, whiskers represent range and boxes indicate lower quartile, median, and upper quartile, from bottom to top. Bar graphs are presented as mean values \pm standard error of the mean (S.E.M.).

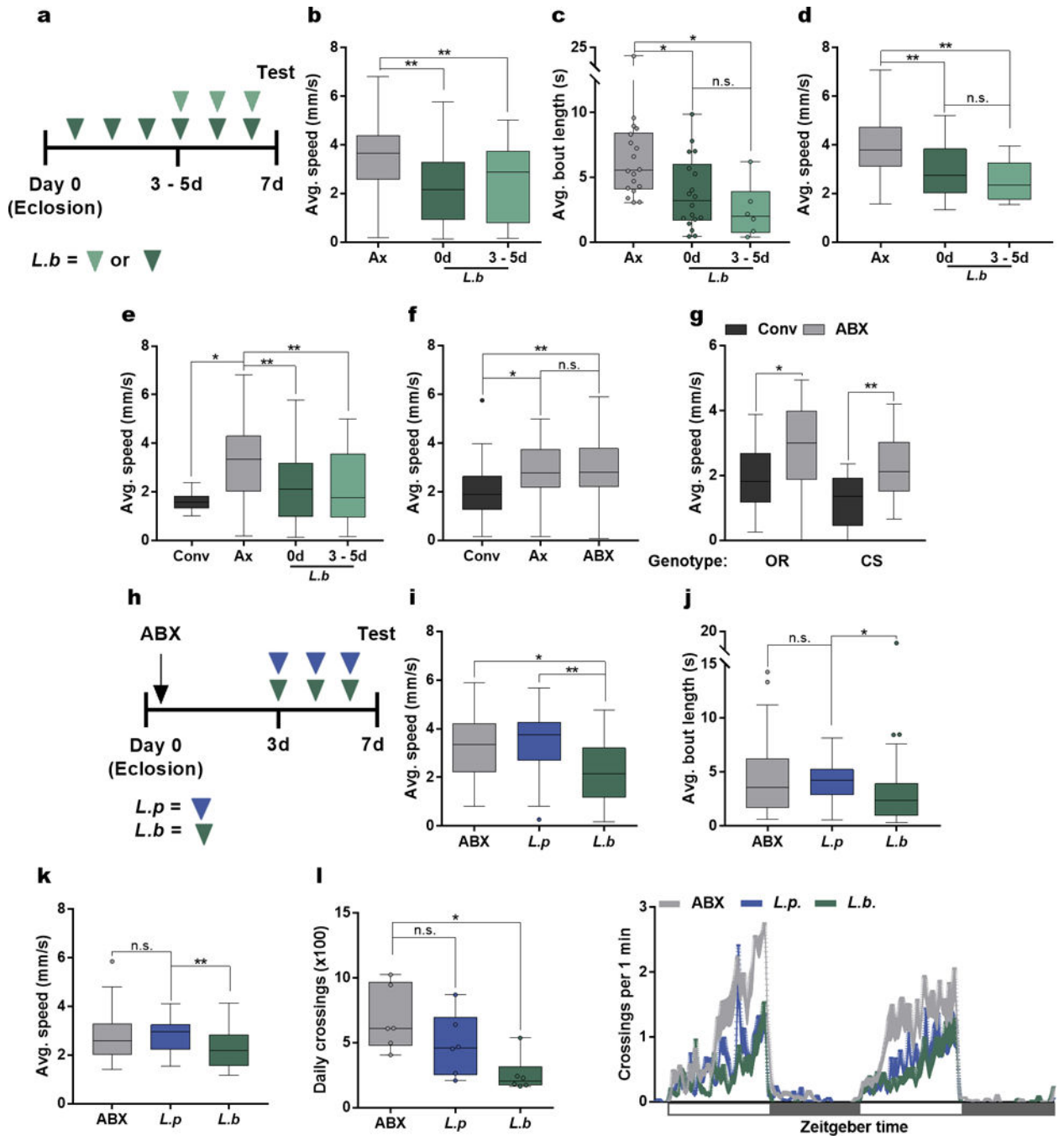
Extended Data



Extended Data Figure 1 | Effects of colonization level, bacterial strain, and host diet on *L. brevis*-modulation of locomotion.

a, Colony forming units (CFU) per individual fly for *L.p* or *L.b* mono-associated flies. Bars represent mean \pm S.E.M. *L.p*, $n = 15$; *L.b*, $n = 18$. **b**, Average speed of Conv, Ax, and *L.b* mono-associated female or male flies. Females: Conv, $n = 90$; Ax, $n = 92$; *L.b*, $n = 89$; Males: Conv, $n = 100$; Ax, $n = 100$; *L.b*, $n = 95$. **c** – **d**, Average speed of Ax or flies mono-associated with *L.b* strains EW, Bb14, or P-2. (**c**) Ax, $n = 58$; *L.b* EW, $n = 57$; *L.b* Bb14, $n =$

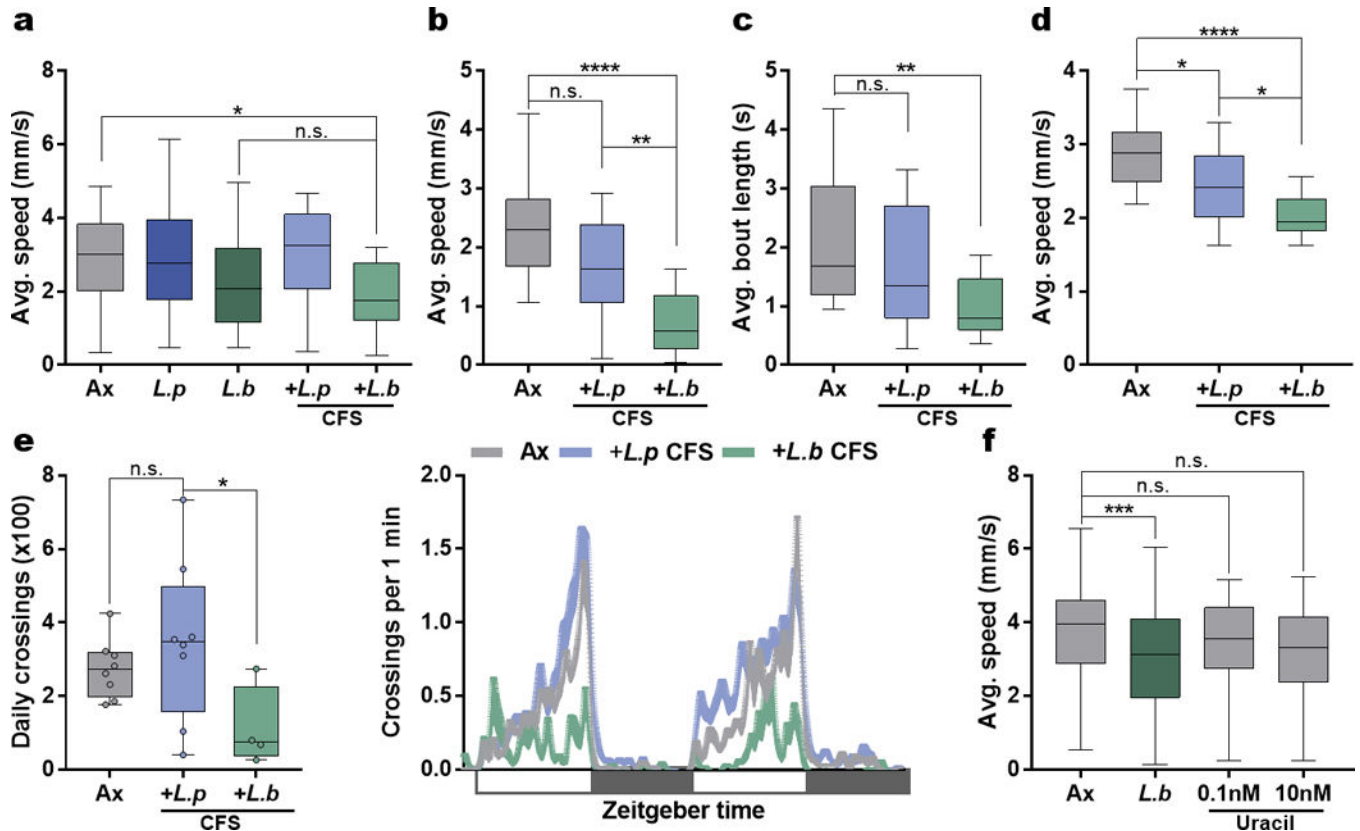
57. **(d)** *Ax*, n = 45; *L.b* EW, n = 28; *L.b* P-2, n = 42. **(e)** Average speed of *Ax* or *L.b* mono-associated flies raised on different diet compositions from eclosion until day 7. Diet 1: *Ax*, n = 20; *L.b*, n = 21; Diet 2: *Ax*, n = 18; *L.b*, n = 16; Diet 3: *Ax*, n = 6; *L.b*, n = 6. **(f)** Average speed during walking bouts for Conv, *Ax*, *L.p*, and *L.b* groups. Conv, n = 23; *Ax*, n = 35; *L.p*, n = 22; *L.b*, n = 22. **(g)** Tripod index for Conv, *Ax*, *L.p*, and *L.b* groups. Conv, n = 6; *Ax*, n = 7; *L.p*, n = 5; *L.b*, n = 5. **(h)** Average speed of *Ax* flies or flies mono-associated with *L.p* or *L.b* alone or in combination (1:1). *Ax*, n = 18; *L.p*, n = 24; *L.b*, n = 24; *L.p+L.b*, n = 24. Box-and-whisker plots show median and IQR. * $P < 0.05$, ** $P < 0.01$, *** $P < 0.001$, **** $P < 0.0001$. Specific P values are in the Supplementary Material. Unpaired Student's t-test (**(a)**), Kruskal-Wallis and Dunn's (**(b – d)** and **(f – h)**), or Mann-Whitney U (**(e)**) post-hoc tests were used for statistical analysis. Data are representative of at least 3 independent trials for each experiment.



Extended Data Figure 2 | Post-eclosion microbial signals decrease host locomotion.

a, Experimental design (**b – e**) in which Ax flies were associated with *L.b* either directly after (day 0, dark green arrows) or 3 – 5 days (light green arrows) following eclosion. **b – d**, Average speed (**b**), average bout length (**c**), and average speed during walking bouts (**d**) of Ax and flies mono-associated with *L.b* at either day 0 or day 3 – 5. (**b**) Ax, n = 46; *L.b* 0d, n = 47; *L.b* 3–5d, n = 43. (**c**) Ax, n = 18; *L.b* 0d, n = 18; *L.b* 3–5d, n = 6. (**d**) Ax, n = 36; *L.b* 0d, n = 36; *L.b* 3–5d, n = 12. **e**, Average speed of Conv, Ax, and flies mono-associated with *L.b* at either day 0 or day 3 – 5. Conv, n = 11; Ax, n = 53; *L.b* 0d, n = 53; *L.b* 3–5d, n = 52.

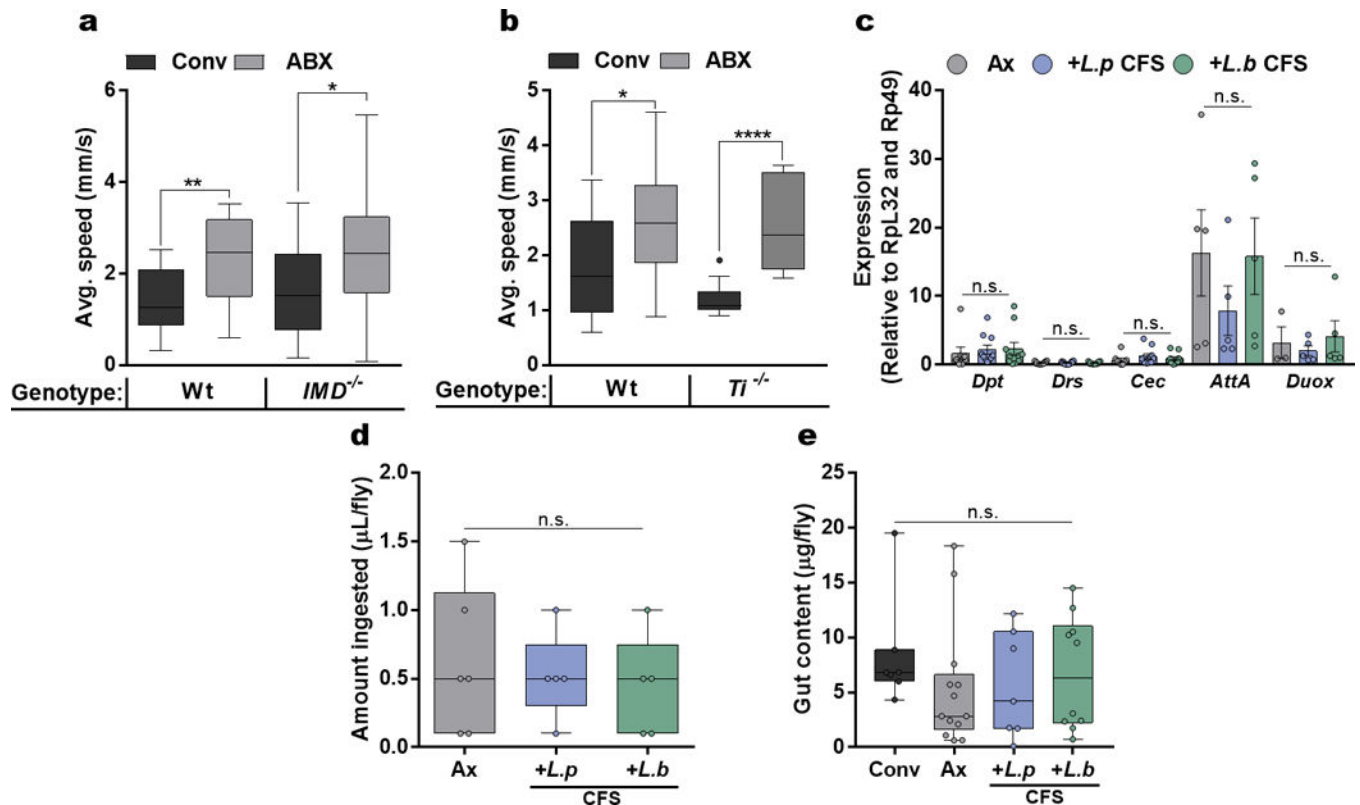
f, Average speed of Conv, Ax, and Conv flies treated with antibiotics for 3 days after eclosion (ABX). Conv, $n = 32$; Ax, $n = 36$; ABX, $n = 36$. **g**, Average speed of Oregon^R (OR) and Canton S (CS) Conv flies and Conv flies treated with antibiotics for 3 days after eclosion (ABX). OR: Conv, $n = 20$; ABX, $n = 22$; CS: Conv, $n = 12$; ABX, $n = 17$. **h**, Experimental design (**i** – **l**) in which conventionally-reared flies were treated with antibiotics (ABX, black arrow) for 3 days following eclosion. All flies were subsequently placed on irradiated media either without supplementation (ABX) or associated with *L.p* (blue arrows) or *L.b* (green arrows) for the 3 days prior to testing. **i** – **k**, Average speed (**i**), average bout length (**j**), and average speed during walking bouts (**k**) calculated for ABX, *L.p*, and *L.b*-associated flies. (**i**) ABX, $n = 29$; *L.p*, $n = 24$; *L.b*, $n = 35$. (**j**) ABX, $n = 36$; *L.p*, $n = 30$; *L.b*, $n = 35$. (**k**) ABX, $n = 42$; *L.p*, $n = 30$; *L.b*, $n = 35$. **l**, Daily activity of ABX, *L.p* and *L.b* groups (virgin female Oregon^R flies) over a 2-day light-dark cycle period each lasting 12 hours, starting at time 0. White boxes represent lights on and gray boxes represent lights off. $n = 6$ /condition. Box-and-whisker plots show median and IQR. * $P < 0.05$, ** $P < 0.01$. Specific P values are in the Supplementary Material. Kruskal-Wallis and Dunn's (**b** – **f** and **i** – **l**) or Mann-Whitney U (**g**) post-hoc tests were used for statistical analysis. Data are representative of at least 2 independent trials for each experiment.



Extended Data Figure 3 | Bacterial-derived products from *L. brevis* alter locomotion.

a, Average speed of Ax, *L.p* or *L.b* mono-associated, and Ax flies treated with cell-free supernatant (CFS) from *L.p* or *L.b*. Ax, $n = 45$; *L.p*, $n = 17$; *L.b*, $n = 42$; *L.p* CFS, $n = 17$; *L.b* CFS, $n = 16$. **b** – **e**, Average speed (**b**), average bout length (**c**), average speed during

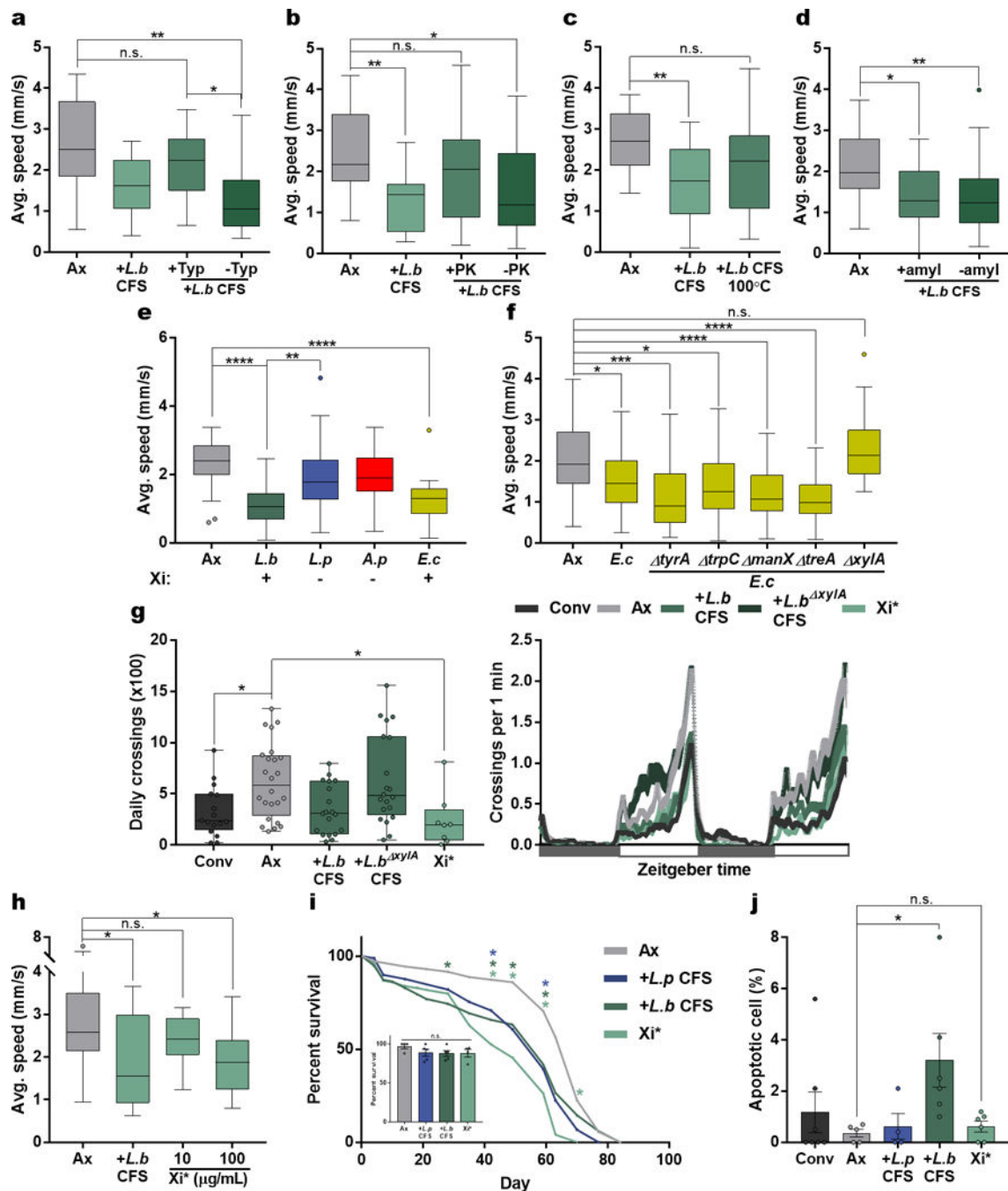
walking bouts (d), and daily activity (e) of Ax and Ax virgin female Oregon^R flies treated with CFS from either *L.p* or *L.b*. White boxes represent lights on and gray boxes represent lights off. (b) Ax, n = 23; *L.p* CFS, n = 20; *L.b* CFS, n = 20. (c) Ax, n = 23; *L.p* CFS, n = 20; *L.b* CFS, n = 17. (d) Ax, n = 22; *L.p* CFS, n = 21; *L.b* CFS, n = 17. (e) Ax, n = 8; *L.p* CFS, n = 8; *L.b* CFS, n = 4. f, Average speed of Ax, *L.b* mono-associated, and Ax uracil-treated flies. Ax, n = 96; *L.b*, n = 88; 0.1 Uracil, n = 41; 10 Uracil, n = 18. Box-and-whisker plots show median and IQR. * $P < 0.05$, ** $P < 0.01$, *** $P < 0.001$, **** $P < 0.0001$. Specific P values are in the Supplementary Material. Kruskal-Wallis and Dunn's post-hoc tests were used for statistical analysis. Data are representative of at least 2 independent trials for each experiment.



Extended Data Figure 4 | Locomotor phenotypes are independent of food intake, anti-microbial peptides, as well as the Immune Deficiency (IMD) and Toll pathways.

a, Average speed of wild-type background (Oregon^R, Wt) and *Imd*^{-/-} flies placed on either media alone or media supplemented with antibiotics (ABX) following eclosion. Wt: Conv, n = 16; ABX, n = 17; *IMD*^{-/-}: Conv, n = 24; ABX, n = 25. **b**, Average speed of wild-type background (Canton S, Wt) and *Ti*^{-/-} flies placed on either media alone or media supplemented with antibiotics (ABX) following eclosion. Wt: Conv, n = 15; ABX, n = 17; *Ti*^{-/-}: Conv, n = 10; ABX, n = 11. **c**, qRT-PCR of immune-related transcripts in Ax and Ax *L.p* or *L.b* CFS treated flies. Bars represent mean \pm S.E.M. *Dpt*: Ax, n = 8; *L.p* CFS, n = 10; *L.b* CFS, n = 10; *Drs*: Ax, n = 10; *L.p* CFS, n = 10; *L.b* CFS, n = 10; *Cec*: Ax, n = 8; *L.p* CFS, n = 10; *L.b* CFS, n = 10; *AttA*: Ax, n = 5; *L.p* CFS, n = 5; *L.b* CFS, n = 5; *Duox*: Ax, n = 3; *L.p* CFS, n = 5; *L.b* CFS, n = 5. **d**, Amount ingested by Ax and Ax *L.p* or *L.b* CFS

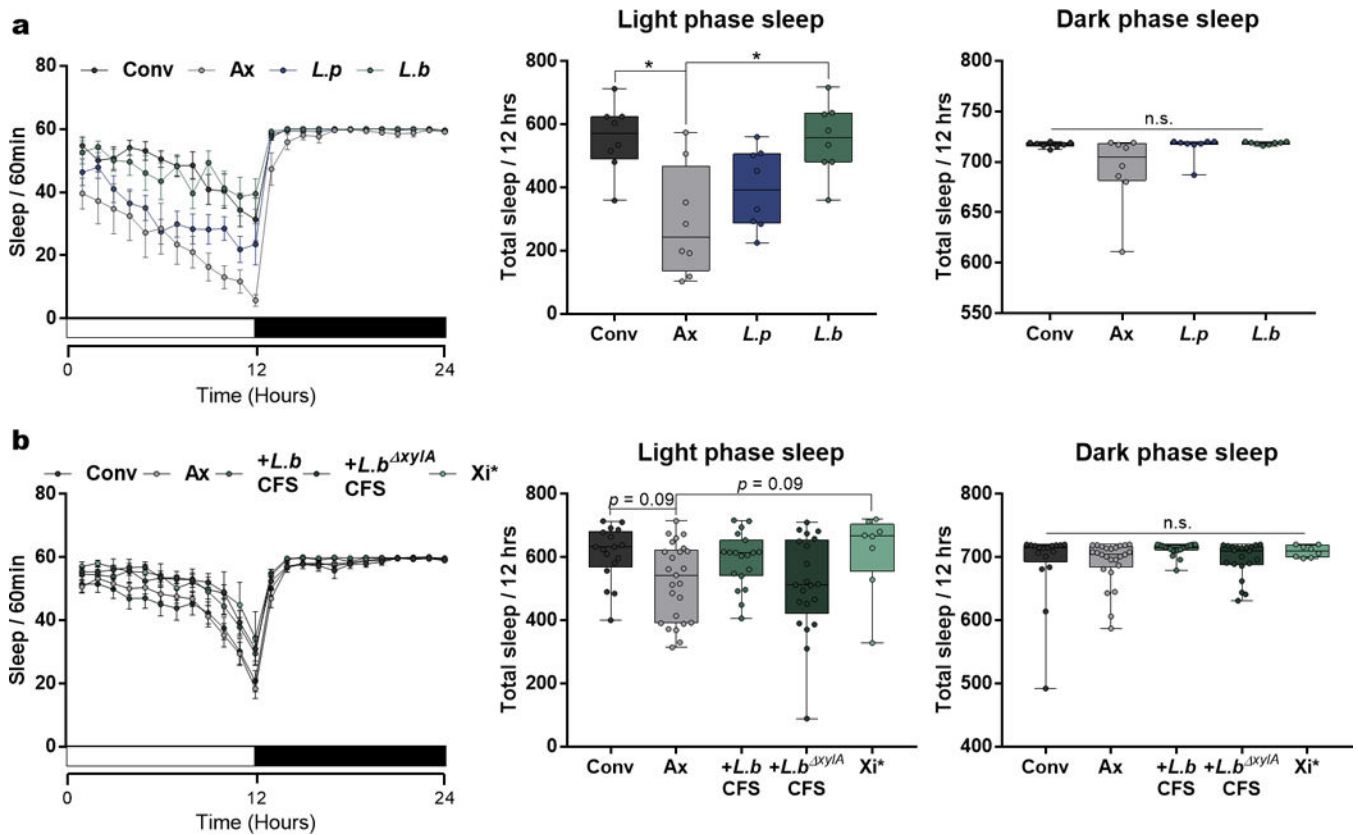
treated flies over 10 trials during MAFE assay. *Ax*, n = 6; *L.p* CFS, n = 5; *L.b* CFS, n = 6. **e**, Intestinal content measured through supplementing the diet of *Conv*, *Ax*, and *L.p* or *L.b* CFS treated *Ax* flies with blue food dye. *Conv*, n = 7; *Ax*, n = 13; *L.p* CFS, n = 7; *L.b* CFS, n = 10. Box-and-whisker plots show median and IQR. * $P < 0.05$, ** $P < 0.01$, **** $P < 0.0001$. Specific P values are in the Supplementary Material. Mann-Whitney $U(\mathbf{a} - \mathbf{b})$, One-way ANOVA and Bonferroni (**c**), or Kruskal-Wallis and Dunn's (**d** - **e**) post-hoc tests were used for statistical analysis. Data are representative of at least 2 independent trials for each experiment. *Dpt*, Dipteracin; *Drs*, Drosomycin; *Cec*, Cecropin; *AttA*, Attacin-A; *Duox*, Dual Oxidase.



Extended Data Figure 5 | Modulation of locomotion by the bacterial enzyme, xylose isomerase.

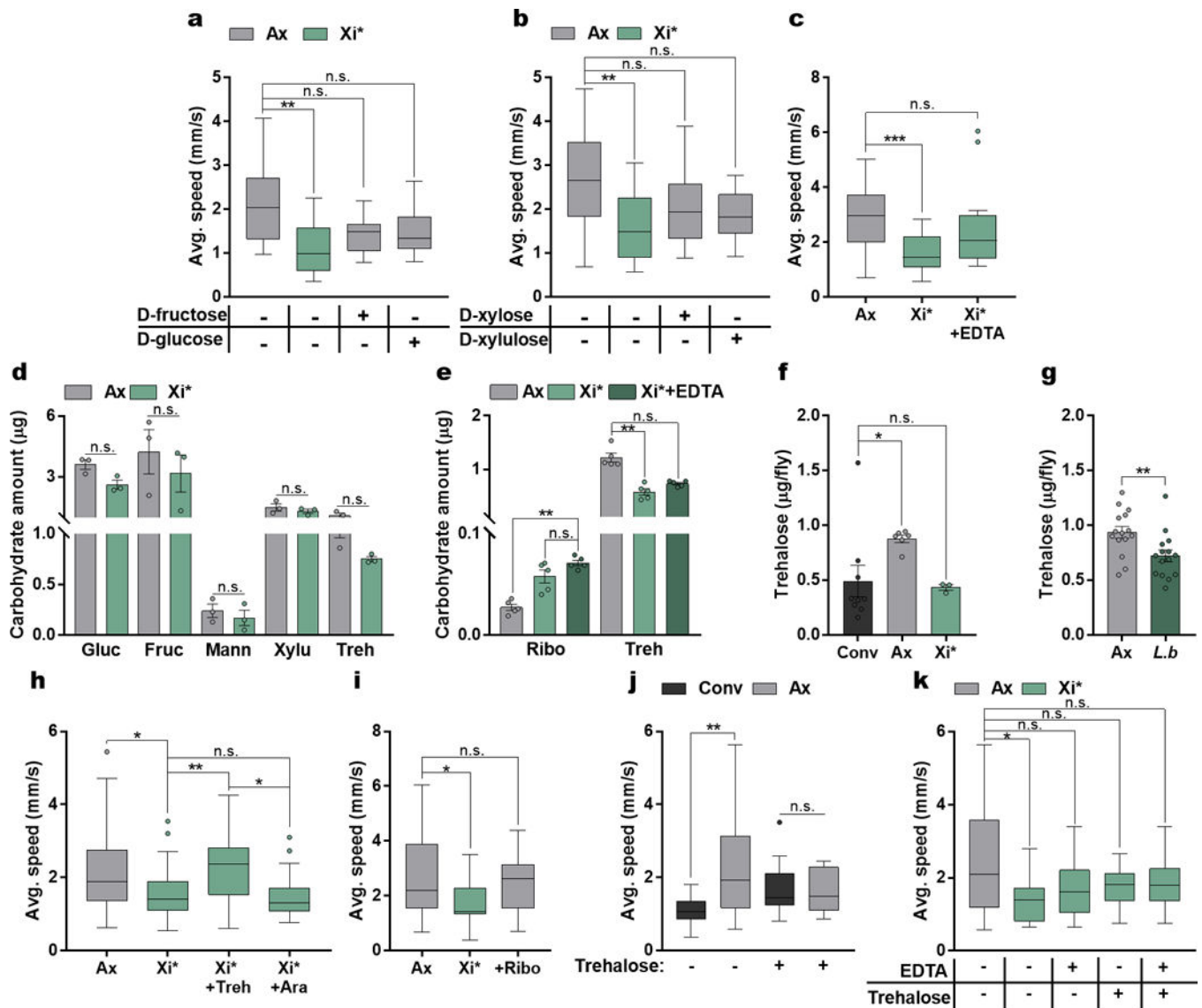
a – c, Average speed of Ax or Ax flies treated with unaltered, protease- (Typ, Trypsin; PK, Proteinase-K), or heat-treated (100°C) *L.b* CFS. **(a)** Ax, n = 18; *L.b* CFS, n = 18; +Typ, n = 17; -Typ, n = 17. **(b)** Ax, n = 23; *L.b* CFS, n = 18; +PK, n = 23; -PK, n = 23. **(c)** n = 18. **d**, Average speed of Ax flies administered with amylase-treated PBS (Ax), amylase-treated *L.b* CFS (+amyl *L.b* CFS), or unaltered *L.b* CFS (-amyl *L.b* CFS). Ax, n = 30; +amyl, n = 17; -amyl, n = 30. **e**, Average speed of Ax flies or flies mono-associated with *L.b*, *L.p*, *A. pomorum* (*A.p*), or *E. coli* (*E.c*). Below shows the presence (+) or absence (-) of Xi based

on NCBI Blastn (*xyIA* locus) and Blastp (Xi) results. Ax, n = 30; *L.b.*, n = 30; *L.p.*, n = 29; *A.p.*, n = 30; *E.c.*, n = 18. **f.** Average speed of Ax and flies mono-associated with either WT *E.c.* or single gene knockout strains of *E.c.* (*tyrA*, *trpC*, *manX*, *treA*, *xyIA*). Ax, n = 65; *E.c.*, n = 52; *E.c.* *tyrA*, n = 18; *E.c.* *trpC*, n = 17; *E.c.* *manX*, n = 45; *E.c.* *treA*, n = 46; *E.c.* *xyIA*, n = 20. **g.** Daily activity of Conv, Ax, and Ax virgin female Oregon^R flies treated with *L.b.* CFS, *L.b.* *xyIA* CFS, or Xi* over a 2-day light-dark cycle period each lasting 12 hours, starting at time 0. White boxes represent lights on and gray boxes represent lights off. Conv, n = 16; Ax, n = 24; *L.b.* CFS, n = 19; *L.b.* *xyIA* CFS, n = 20; Xi*, n = 8. **h.** Average speed of Ax and Ax flies treated with *L.b.* CFS or Xi*. Ax, n = 16; *L.b.* CFS, n = 11; 10 µg/mL Xi*, n = 12; 100 µg/mL Xi*, n = 14. **i.** Lifespan measurements for Ax and Ax treated with *L.p.* CFS, *L.b.* CFS, or Xi*. Asterisks above represent significance at the time point measured by Kruskal-Wallis and Dunn's post-hoc test. Inset image shows survival at day 7, error bars represent mean ± S.E.M. Ax, n = 4 groups; *L.p.* CFS, n = 5 groups; *L.b.* CFS, n = 5 groups; Xi*, n = 4 groups. **j.** Percentage of apoptotic cells in the intestine of Conv, Ax, and Ax treated with *L.p.* CFS, *L.b.* CFS, or Xi*. Bars represent mean ± S.E.M. Conv, n = 7; Ax, n = 5; *L.p.* CFS, n = 4; *L.b.* CFS, n = 6; Xi*, n = 6. Box-and-whisker plots show median and IQR. * $P < 0.05$, ** $P < 0.01$, *** $P < 0.001$, **** $P < 0.0001$. Specific P values are in the Supplementary Material. Kruskal-Wallis and Dunn's (**a** – **i**) or Log-rank (**i**) post-hoc tests were used for statistical analysis. Data are representative of at least 2 independent trials for each experiment.



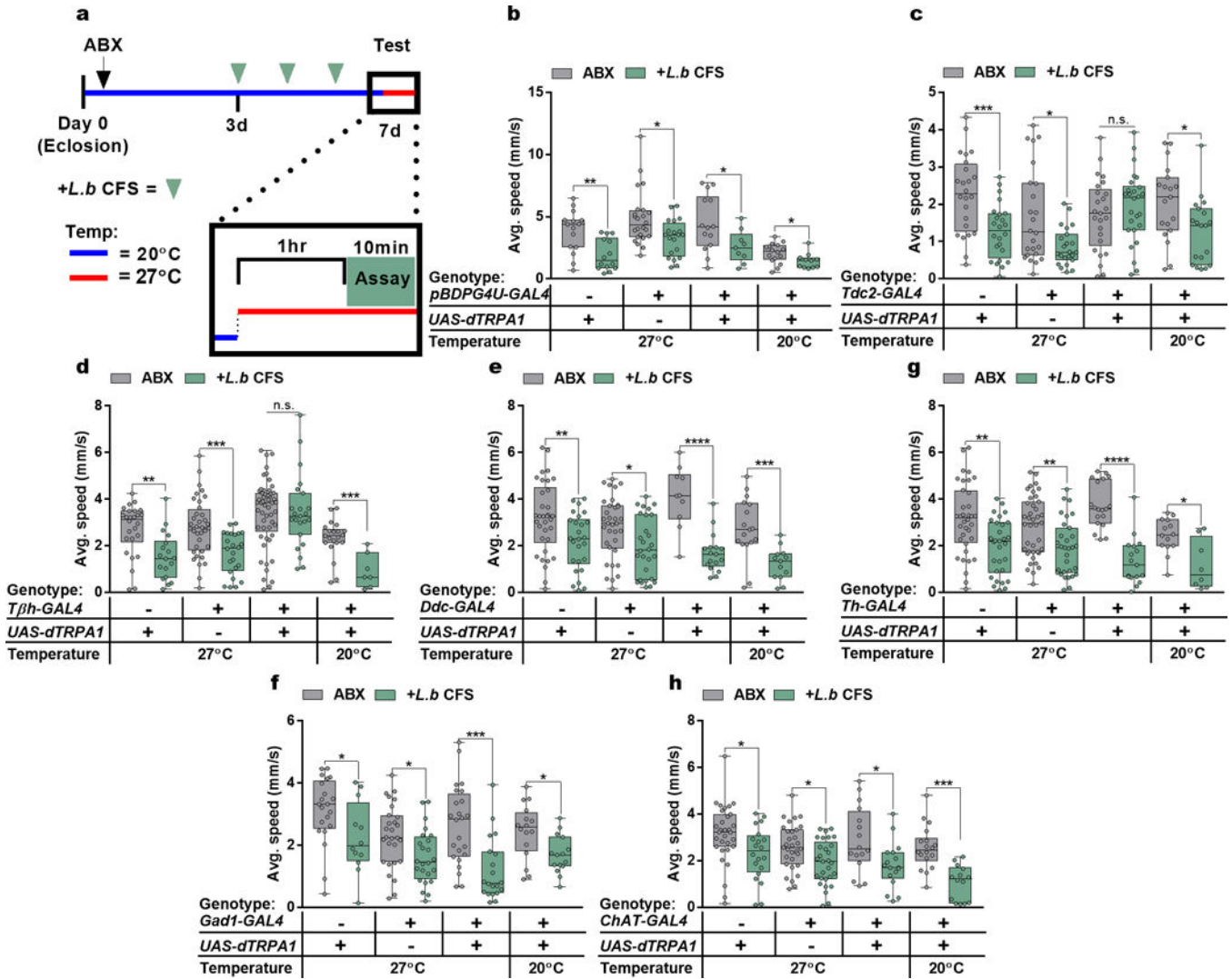
Extended Data Figure 6 | Sleep analysis for mono-colonized flies and flies administered with bacteria factors.

a, 24-hour sleep profiles of Conv, Ax, *L.p.*-, and *L.b.*-colonized virgin female Oregon^R flies with the number of sleep bouts in 60 min time window and total sleep in the light or dark phase. Error bars represent mean \pm S.E.M. $n = 8$ /condition. **b**, 24-hour sleep profiles of Conv, Ax, *L.b* CFS-, *L.b xy1A* CFS-, and Xi* treated Ax virgin female Oregon^R flies with the number of sleep bouts in 60 min time window and total sleep in the light or dark phase. Error bars represent mean \pm S.E.M. Conv, $n = 17$; Ax, $n = 25$; *L.b* CFS-, $n = 19$; *L.b xy1A* CFS-, $n = 21$; Xi*, $n = 8$. Box-and-whisker plots show median and IQR. * $P < 0.05$. Specific P values are in the Supplementary Material. Kruskal-Wallis and Dunn's post-hoc tests were used for statistical analysis. Data are representative of at least 2 independent trials for each experiment.



Extended Data Figure 7 | Xylose isomerase activity and key carbohydrates are involved in Xi-mediated changes in locomotion.

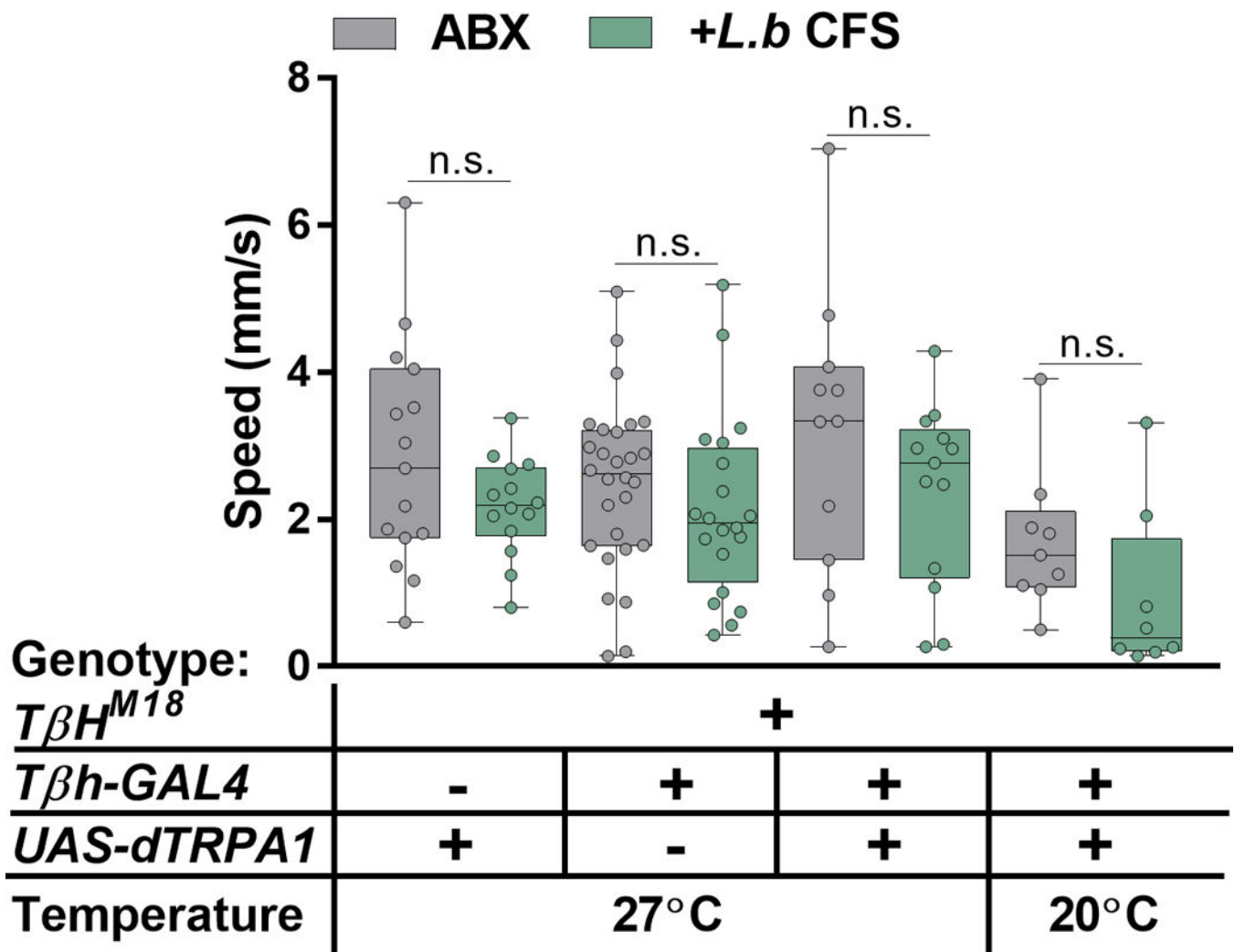
a – b, Average speed of Ax and Xi* flies treated with Xi* or 100 µg of D-fructose, D-glucose, D-xylose, or D-xylulose. **(a)** Ax, n = 16; Xi*, n = 13; D-fructose, n = 13; D-glucose, n = 15. **(b)** Ax, n = 26; Xi*, n = 21; D-xylose, n = 22; D-xylulose, n = 18. **c**, Average speed of Ax and Xi* flies treated with either Xi* or Xi* inactivated through treatment with 5mM EDTA. Ax, n = 21; Xi*, n = 16; Xi*+EDTA, n = 18. **d**, Carbohydrate levels in Ax and Xi*-treated fly media. Each sample is from 0.1 g of fly media and represents a separate vial. Bars represent mean \pm S.E.M. n = 3 samples/condition. **e**, Carbohydrate levels in Ax, Xi*, and EDTA-treated Xi* flies. Each sample contains 5 flies. Bars represent mean \pm S.E.M. n = 5 samples/condition. **f**, Trehalose levels in Conv, Ax, and Xi*-treated flies. Bars represent mean \pm S.E.M. Conv, n = 9 samples; Ax, n = 6 samples; Xi*, n = 3 samples. **g**, Trehalose levels in Ax and *L.b* colonized flies. Bars represent mean \pm S.E.M. n = 15 samples/condition. **h**, Average speed of Ax and Xi*-treated flies supplemented with either trehalose (Treh, 10 mg/mL) or arabinose (Ara, 10 mg/mL) for 3 days before testing. Ax, n = 40; Xi*, n = 40; Xi*+Treh, n = 39; Xi*+Ara, n = 18. **i**, Average speed of Ax, Xi*-, or ribose- (Ribo, 10 mg/mL) treated flies. Ax, n = 29; Xi*, n = 25; Ribo, n = 12. **j**, Average speed of Conv and Ax flies supplemented with trehalose (Treh, 10 mg/mL) for 3 days before testing. Conv, n = 15; Ax, n = 22; Conv+Treh, n = 18; Ax+Treh, n = 15. **k**, Average speed of Ax and Xi* or EDTA-treated Xi* Ax flies subsequently left untreated or supplemented with trehalose (Treh, 10 mg/mL) for 3 days before testing. Ax, n = 27; Xi, n = 19; Xi+EDTA, n = 24; Xi+Treh, n = 19; Xi+EDTA+Treh, n = 25. Box-and-whisker plots show median and IQR. * $P < 0.05$, ** $P < 0.01$, *** $P < 0.001$. Specific P values are in the Supplementary Material. Kruskal-Wallis and Dunn's (**a – c**, **e – f**, **h – k**) or a Mann-Whitney U (**d** and **g**) post-hoc tests were used for statistical analysis. Data are representative of at least 2 independent trials for each experiment. Gluc, glucose; Fruc, fructose; Mann, mannose; Xylu, xylulose; Treh, trehalose; Ribo, ribose.



Extended Data Figure 8 | Thermogenetic activation of neuromodulator-GAL4 lines.

a, Experimental design in which Conv flies (Canton-S) were treated with antibiotics (ABX, black arrow) for 3 days following eclosion. All flies were subsequently placed on irradiated media either without supplementation or treated with *L.b* CFS (green arrows) for 3 days. 1 hr. prior to and during testing flies were either exposed to 27°C (red line) to facilitate thermogenetic activation or kept at 20°C (blue line). **b – h**, Average speed of flies previously treated with antibiotics and subsequently left untreated (ABX) or administered with *L.b* CFS for 3 days prior to testing. (**b**) UAS: ABX, n = 15; *L.b* CFS, n = 14; GAL4: ABX, n = 24; *L.b* CFS, n = 20; GAL4>UAS (27°C): ABX, n = 14; *L.b* CFS, n = 9; GAL4>UAS (20°C): ABX, n = 16; *L.b* CFS, n = 11. (**c**) UAS: ABX, n = 24; *L.b* CFS, n = 24; GAL4: ABX, n = 24; *L.b* CFS, n = 23; GAL4>UAS (27°C): ABX, n = 25; *L.b* CFS, n = 26; GAL4>UAS (20°C): ABX, n = 19; *L.b* CFS, n = 19. (**d**) UAS: ABX, n = 26; *L.b* CFS, n = 18; GAL4: ABX, n = 36; *L.b* CFS, n = 24; GAL4>UAS (27°C): ABX, n = 53; *L.b* CFS, n = 23; GAL4>UAS (20°C): ABX, n = 21; *L.b* CFS, n = 7. (**e**) UAS: ABX, n = 34; *L.b* CFS, n = 26; GAL4: ABX, n = 34; *L.b* CFS, n = 28; GAL4>UAS (27°C): ABX, n = 10; *L.b* CFS, n = 17;

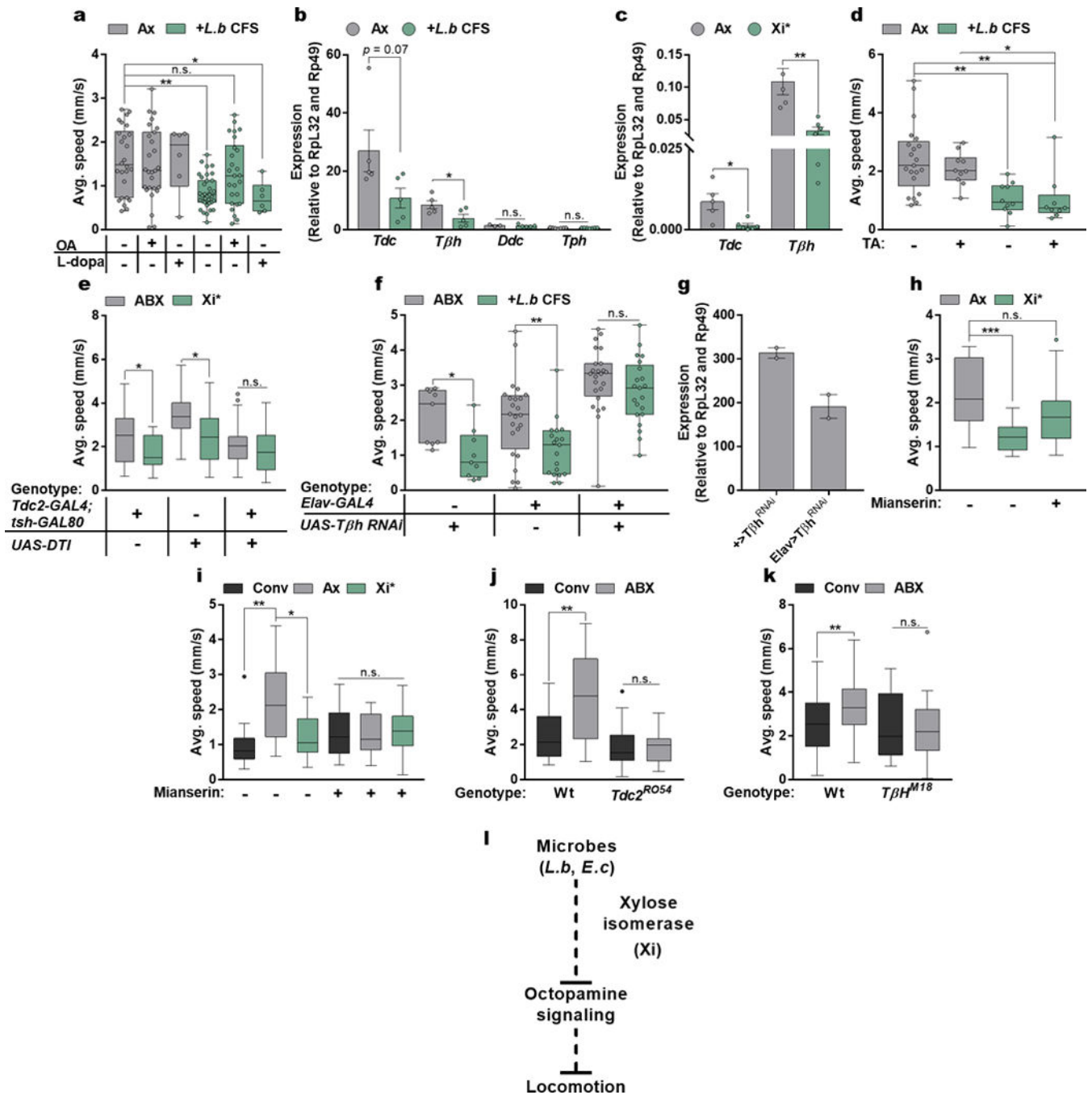
GAL4>UAS (20°C): ABX, n = 17; *L.b* CFS, n = 13. (f) UAS: ABX, n = 36; *L.b* CFS, n = 30; GAL4: ABX, n = 40; *L.b* CFS, n = 31; GAL4>UAS (27°C): ABX, n = 19; *L.b* CFS, n = 17; GAL4>UAS (20°C): ABX, n = 14; *L.b* CFS, n = 8. (g) UAS: ABX, n = 21; *L.b* CFS, n = 12; GAL4: ABX, n = 28; *L.b* CFS, n = 24; GAL4>UAS (27°C): ABX, n = 24; *L.b* CFS, n = 20; GAL4>UAS (20°C): ABX, n = 16; *L.b* CFS, n = 15. (h) UAS: ABX, n = 31; *L.b* CFS, n = 20; GAL4: ABX, n = 31; *L.b* CFS, n = 29; GAL4>UAS (27°C): ABX, n = 16; *L.b* CFS, n = 17; GAL4>UAS (20°C): ABX, n = 18; *L.b* CFS, n = 14. Box-and-whisker plots show median and IQR. * $P < 0.05$, ** $P < 0.01$, *** $P < 0.001$, **** $P < 0.0001$. Specific P values are in the Supplementary Material. Mann-Whitney U post-hoc tests following a Two-way ANOVA were used for statistical analysis. Data are representative of at least 2 independent trials for each experiment.



Extended Data Figure 9 | Activation of octopaminergic neurons in flies carrying a null allele for $T\beta h$ ($T\beta H^{M18}$).

Average speed of flies previously treated with antibiotics and subsequently left untreated (ABX) or administered with *L.b* CFS for 3 days prior to testing. UAS: ABX, n = 15; *L.b* CFS, n = 14; GAL4: ABX, n = 28; *L.b* CFS, n = 20; GAL4>UAS (27°C): ABX, n = 11; *L.b*

CFS, $n = 13$; GAL4>UAS (20°C): ABX, $n = 9$; *L.b* CFS, $n = 8$. Box-and-whisker plots show median and IQR. Specific *P* values are in the Supplementary Material. Mann-Whitney *U* post-hoc tests following a Two-way ANOVA were used for statistical analysis. Data are representative of at least 2 independent trials.



Extended Data Figure 10]. Octopamine mediates *L. brevis*- and xylose isomerase-induced changes in locomotion.

a. Average speed of Ax and *L.b* CFS-treated Ax flies left untreated or supplemented with octopamine (OA, 10 mg/mL) or L-dopa (1 mg/mL) for 3 days. Ax, $n = 26$; Ax+OA, $n = 27$;

Ax+L-dopa, n = 6; *L.b* CFS, n = 35; *L.b* CFS+OA, n = 26; *L.b* CFS+L-dopa, n = 6. **b**, qRT-PCR for transcripts from heads of Ax and *L.b* CFS-treated Ax flies. Bars represent mean \pm S.E.M. *Tdc*: n = 5; *T β h*, n = 5; *Ddc*: Ax, n = 3; *L.b* CFS, n = 5; *Tph*: n = 7. **c**, qRT-PCR for transcripts from heads of Ax or Ax Xi*-treated flies. Bars represent mean \pm S.E.M. Ax, n = 5 samples; Xi*, n = 6 samples. **d**, Average speed of Ax and *L.b* CFS-treated Ax flies left untreated or supplemented with tyramine (TA, 10 mg/mL) for 3 days. Ax, n = 21; Ax+TA, n = 10; *L.b* CFS, n = 10; *L.b* CFS+TA, n = 9. **e**, Average speed of control lines and flies expressing *DTI* in octopaminergic and tyraminerbic neurons outside of the ventral nerve cord. All flies were previously treated with antibiotics and subsequently left untreated (ABX) or administered with Xi* for 3 days prior to testing. GAL4;GAL80: Ax, n = 25; Xi*, n = 18; UAS: Ax, n = 26; Xi*, n = 21; GAL4>UAS: Ax, n = 39; Xi*, n = 23. **f**, Average speed of control lines and flies expressing T β h RNAi in all neurons. All flies were previously treated with antibiotics and subsequently left untreated (ABX) or administered with *L.b* CFS for 3 days prior to testing. UAS: n = 9; GAL4: Ax, n = 24; *L.b* CFS, n = 19; GAL4>UAS: Ax, n = 24; *L.b* CFS, n = 21. **g**, T β h mRNA measured from heads of flies previously treated with antibiotics. Error bars represent range. n = 2 samples/condition. **h**, Average speed of Ax and Xi*-treated Ax flies left untreated or supplemented with mianserin (2 mg/mL) for 3 days. Ax, n = 14; Xi*, n = 15; Xi*+Mian, n = 15. **i**, Average speed of Conv, Ax, and Xi*-treated Ax flies left untreated or supplemented with mianserin (2 mg/mL) for 3 days. Conv, n = 13; Ax, n = 28; Xi*, n = 24; Conv+Mian, n = 27; Ax+Mian, n = 22; Xi*+Mian, n = 22. **j**, Average speed of wild-type background (w+, Wt) and *Tdc2* null mutants (*Tdc2^{RO54}*) either left untreated or after treatment with antibiotics for 3 days following eclosion. Wt Conv, n = 13; Wt ABX, n = 21; *Tdc^{RO54}* Conv, n = 28; *Tdc^{RO54}* ABX, n = 34. **k**, Average speed of wild-type background (Canton-S, Wt) and T β h null mutants (*T β H^{M18}*) either left untreated or after treatment with antibiotics for 3 days following eclosion. Wt Conv, n = 38; Wt ABX, n = 42; *T β H^{M18}* Conv, n = 25; *T β H^{M18}* ABX, n = 33. **l**, Model of bacterial modulation of host locomotion. Box-and-whisker plots show median and IQR. * $P < 0.05$, ** $P < 0.01$, *** $P < 0.001$. Specific P values are in the Supplementary Material. Kruskal-Wallis and Dunn's (a, d, h – i), unpaired Student's t-test (b – c and g), or Mann-Whitney U (e – f and j – k) post-hoc tests were used for statistical analysis. Data are representative of at least 2 independent trials for each experiment. *Tdc*, Tyrosine decarboxylase; *T β h*, Tyramine beta-hydroxylase; *Ddc*, DOPA decarboxylase; *Tph*, Tryptophan hydroxylase.

Supplementary Material

Refer to Web version on PubMed Central for supplementary material.

Acknowledgements

We thank Drs. H. Chu, G. Sharon, W.-L. Wu, J. K. Scarpa, and E. D. Hoopfer as well as the Mazmanian laboratory for helpful critiques. We are grateful to Drs. A. A. Aravin (Caltech), and K. Fejes Tóth (Caltech) for use of their laboratory space. We thank Drs. D. J. Anderson (Caltech), H. A. Lester (Caltech), V. Gradinaru (Caltech), and M.-F. Chesselet (UCLA) for helpful discussions. We also thank A. R. Sandoval, M. Meyerowitz, and M. Smalley for technical support and Y. Garcia-Flores for administrative support. We are grateful to Dr. D. C. Hall for creating custom python scripts. We thank Dr. W.-J. Lee (Seoul National University) for the *L. brevis*^{EW}, *L. plantarum*^{WJL}, and *A. pomorum* bacterial strains, the Yale Coli Genetic Stock Center for wild type and mutant *E. coli* strains, and Drs. M. H. Dickinson (Caltech), D. J. Anderson (Caltech), A. A. Aravin (Caltech), and K. Fejes Tóth (Caltech) for

fly lines. We thank the GlycoAnalytics Core (UCSD) for their help with carbohydrate analysis. We are also grateful to Drs. M. Fischbach (Stanford), and M. Funabashi (Stanford) for the pGID023 vector, and helpful advice. Imaging was performed in the Biological Imaging Facility, with the support of the Caltech Beckman Institute and the Arnold and Mabel Beckman Foundation. C.E.S. was partially supported by the Center for Environmental Microbial Interactions at Caltech. This project was funded by grants from the NIH (NS085910) and the Heritage Medical Research Institute to S.K.M.

References

1. Diaz Heijtz R, et al. Normal gut microbiota modulates brain development and behavior. *Proc. Natl. Acad. Sci.* 108, 3047–52 (2011). [PubMed: 21282636]
2. Bravo JA, et al. Ingestion of *Lactobacillus* strain regulates emotional behavior and central GABA receptor expression in a mouse via the vagus nerve. *Proc. Natl. Acad. Sci.* 108, 16050–16055 (2011). [PubMed: 21876150]
3. Luczynski P, et al. Microbiota regulates visceral pain in the mouse. *Elife.* 6, e25887 (2017). [PubMed: 28629511]
4. Gacias M et al. Microbiota-driven transcriptional changes in prefrontal cortex override genetic differences in social behavior. *Elife.* 5, e13442 (2016). [PubMed: 27097105]
5. Fischer C et al. Metabolite exchange between microbiome members produces compounds that influence *Drosophila* behavior. *Elife.* 6, 1–25 (2017).
6. Leitão- Goncalves R, et al. Commensal bacteria and essential amino acids control food choice behavior and reproduction. *PLoS Biol.* 15, 1–29 (2016).
7. Wong ACN et al. Gut microbiota modifies olfactory-guided microbial preferences and foraging decisions in *Drosophila*. *Curr. Biol.* 27, 2397–2404.e4 (2017). [PubMed: 28756953]
8. Liu W, et al. Enterococci mediate the oviposition preference of *Drosophila melanogaster* through sucrose catabolism. *Sci. Rep.* 7, 1–14 (2017). [PubMed: 28127051]
9. Sharon G et al. Commensal bacteria play a role in mating preference of *Drosophila melanogaster*. *Proc. Natl. Acad. Sci.* 107, 20051–20056 (2010). [PubMed: 21041648]
10. Huston SJ & Jayaraman V Studying sensorimotor integration in insects. *Curr. Opin. Neurobiol.* 21, 527–34 (2011). [PubMed: 21705212]
11. Dickinson MH, et al. How animals move: an integrative view. *Science.* 288, 100–106 (2000). [PubMed: 10753108]
12. Pearson KG Common principles of motor control in vertebrates and invertebrates. *Annu. Rev. Neurosci.* 16, 265–297 (1993). [PubMed: 8460894]
13. Strausfeld NJ & Hirth F Deep homology of arthropod central complex and vertebrate basal ganglia. *Science.* 340, 157–161 (2013). [PubMed: 23580521]
14. Martin JR, Ernst R & Heisenberg M Temporal pattern of locomotor activity in *Drosophila melanogaster*. *J. Comp. Physiol.* 184, 73–84 (1999). [PubMed: 10077864]
15. Erkosar B, Storelli G, Defaye A & Leulier F Host-intestinal microbiota mutualism: “learning on the fly.” *Cell Host Microbe.* 13, 8–14 (2013). [PubMed: 23332152]
16. Wong ACN, Ng P & Douglas AE Low-diversity bacterial community in the gut of the fruitfly *Drosophila melanogaster*. *Environ. Microbiol.* 13, 1889–900 (2011). [PubMed: 21631690]
17. Schwarzer M, et al. *Lactobacillus plantarum* strain maintains growth of infant mice during chronic undernutrition. *Science.* 351, 854–857 (2016). [PubMed: 26912894]
18. Lee K-A et al. Bacterial-derived uracil as a modulator of mucosal immunity and gut-microbe homeostasis in *Drosophila*. *Cell.* 153, 797–811 (2013). [PubMed: 23663779]
19. Lemaitre B & Miguel-Aliaga I The digestive tract of *Drosophila melanogaster*. *Annu. Rev. Genet.* 47, 377–404 (2013). [PubMed: 24016187]
20. Kimura KI & Truman JW Postmetamorphic cell death in the nervous and muscular systems of *Drosophila melanogaster*. *J. Neurosci.* 10, 403–401 (1990). [PubMed: 2106014]
21. Tissot M & Stocker RF Metamorphosis in *Drosophila* and other insects: The fate of neurons throughout the stages. *Prog. Neurobiol.* 62, 89–111 (2000). [PubMed: 10821983]
22. Blacher E, Levy M, Tatirovsky E & Elinav E Microbiome-modulated metabolites at the interface of host immunity. *J. Immunol.* 198, 572–580 (2017). [PubMed: 28069752]

23. Breton J, et al. Gut commensal *E. coli* proteins activate host satiety pathways following nutrient-induced bacterial growth. *Cell Metab.* 23, 1–11 (2016). [PubMed: 26698916]
24. Mann K, Gordon M & Scott K A pair of interneurons influences the choice between feeding and locomotion in *Drosophila*. *Neuron.* 79, 754–765 (2013). [PubMed: 23972600]
25. Wong AC-N, Dobson AJ & Douglas AE Gut microbiota dictates the metabolic response of *Drosophila* to diet. *J. Exp. Biol.* 217, 1894–901 (2014). [PubMed: 24577449]
26. Kim E-K, Park YM, Lee OY, & Lee W-J Draft Genome Sequence of *Lactobacillus brevis* Strain EW, a *Drosophila* Gut Pathobiont. *Genome Announc.* 1, e00938–13 (2013). [PubMed: 24265492]
27. Martino ME, et al. Resequencing of the *Lactobacillus plantarum* Strain WJL Genome. *Genome Announc.* 3, e01382–15 (2015). [PubMed: 26607892]
28. Baba T et al. Construction of *Escherichia coli* K-12 in-frame, single-gene knockout mutants: the Keio collection. *Mol. Syst. Biol.* 2, 2006008 (2006).
29. Yamanaka K Purification, crystallization, and properties of the D-xylose isomerase from *Lactobacillus brevis*. *Biochim. Biophys. Acta* 151, 670–80 (1967).
30. Ridley EV, Wong ACN, Westmiller S & Douglas AE Impact of the resident microbiota on the nutritional phenotype of *Drosophila melanogaster*. *PLoS One* 7, e36765 (2012). [PubMed: 22586494]
31. Yang Z et al. Octopamine mediates starvation-induced hyperactivity in adult *Drosophila*. *Proc. Natl. Acad. Sci.* 112, 5219–5224 (2015). [PubMed: 25848004]
32. Chen A et al. Dispensable, redundant, complementary, and cooperative roles of dopamine, octopamine, and serotonin in *Drosophila melanogaster*. *Genetics.* 193, 159–76 (2013). [PubMed: 23086220]
33. Riemensperger T, et al. Behavioral consequences of dopamine deficiency in the *Drosophila* central nervous system. *Proc. Natl. Acad. Sci.* 108, 834–839 (2011). [PubMed: 21187381]
34. Mithieux G, et al. Portal sensing of intestinal gluconeogenesis is a mechanistic link in the diminution of food intake induced by diet protein. *Cell Metab.* 2, 321–329 (2005). [PubMed: 16271532]
35. Hamada FN, et al. An internal thermal sensor controlling temperature preference in *Drosophila*. *Nature.* 454, 217–220 (2008). [PubMed: 18548007]
36. Roeder T Tyramine and octopamine: ruling behavior and metabolism. *Annu. Rev. Entomol.* 50, 447–477 (2005). [PubMed: 15355245]
37. Crocker A & Sehgal A Octopamine regulates sleep in *Drosophila* through protein kinase A-dependent mechanisms. *J. Neurosci.* 38, 9377–9385 (2008).
38. Crocker A, Shahidullah M, Levitan IB & Sehgal A Identification of a neural circuit that underlies the effects of octopamine on sleep:wake behavior. *Neuron.* 65, 670–681 (2010). [PubMed: 20223202]
39. Selcho M, Pauls D, El Jundi B, Stocker RF & Thum AS The role of octopamine and tyramine in *Drosophila* larval locomotion. *J. Comp. Neurol.* 520, 3764–3785 (2012). [PubMed: 22627970]
40. Saraswati S, Fox LE, Soll DR & Wu CF Tyramine and octopamine have opposite effects on the locomotion of *Drosophila* larvae. *J. Neurobiol.* 58, 425–441 (2004). [PubMed: 14978721]
41. Klaassen LW & Kammer AE Octopamine enhances neuromuscular transmission in developing and adult moths, *Manduca sexta*. *J. Neurobiol.* 16, 227–243 (1985). [PubMed: 2989425]
42. Weisel-Eichler A & Libersat F Neuromodulation of flight initiation by octopamine in the cockroach *Periplaneta americana*. *J. Comp. Physiol. A.* 179, 103–112 (1996).
43. Brembs B, Christiansen F, Pflugger HJ & Duch C Flight initiation and maintenance deficits in flies with genetically altered biogenic amine levels. *J. Neurosci.* 27, 11122–11131 (2007). [PubMed: 17928454]
44. van Breugel F, Suver MP & Dickinson MH Octopaminergic modulation of the visual flight speed regulator of *Drosophila*. *J. Exp. Biol.* 217, 1737–1744 (2014). [PubMed: 24526725]
45. Han DD, Stein D & Stevens LM Investigating the function of follicular subpopulations during *Drosophila* oogenesis through hormone-dependent enhancer-targeted cell ablation. *Development* 127, 573–83 (2000). [PubMed: 10631178]

46. Selkrig J et al. The *Drosophila* microbiome has a limited influence on sleep, activity, and courtship behaviors. *Sci Rep* 8, 10646 (2018). [PubMed: 30006625]
47. Nishino R et al. Commensal microbiota modulate murine behaviors in a strictly contamination-free environment confirmed by culture-based methods. *Neurogastroenterol. Motil.* 25, 521–528 (2013). [PubMed: 23480302]
48. Lendrum JE, Seebach B, Klein B & Liu S Sleep and the gut microbiome: antibiotic-induced depletion of the gut microbiota reduces nocturnal sleep in mice. *bioRxiv.* (2017).
49. Berridge CW Noradrenergic modulation of arousal. *Brain Res. Rev.* 58, 1–17 (2008). [PubMed: 18199483]
50. Monastirioti M, Linn CE, & White K Characterization of *Drosophila* tyramine beta-hydroxylase gene and isolation of mutant flies lacking octopamine. *J. Neurosci.* 16, 3900–3911 (1996). [PubMed: 8656284]
51. Clyne JD & Miesenbock G Sex-specific control and tuning of the pattern generator for courtship song in *Drosophila*. *Cell.* 133, 354–363 (2008). [PubMed: 18423205]
52. Shiga Y, Tanaka-Matakatsu M, & Hayashi S A nuclear GFP/ beta-galactosidase fusion protein as a marker for morphogenesis in living *Drosophila*. *Dev. Growth Differ.* 38, 99–106 (1996).
53. Lee WC & Micchelli CA Development and characterization of a chemically defined food for *Drosophila*. *PLoS One.* 8, 1–10 (2013).
54. Brummel T, Ching A, Seroude L, Simon AF & Benzer S *Drosophila* lifespan enhancement by exogenous bacteria. *Proc. Natl. Acad. Sci.* 101, 12974–12979 (2004). [PubMed: 15322271]
55. Ren C, Webster P, Finkel SE & Tower J Increased internal and external bacterial load during *Drosophila* aging without life-span trade-off. *Cell Metab.* 6, 144–52 (2007). [PubMed: 17681150]
56. Ryu J-H, et al. Innate immune homeostasis by the homeobox gene caudal and commensal-gut mutualism in *Drosophila*. *Science.* 319, 777–82 (2008). [PubMed: 18218863]
57. Storelli G, et al. *Lactobacillus plantarum* promotes *Drosophila* systemic growth by modulating hormonal signals through TOR-dependent nutrient sensing. *Cell Metab.* 14, 403–14 (2011). [PubMed: 21907145]
58. Shin SC, et al. *Drosophila* microbiome modulates host developmental and metabolic homeostasis via insulin signaling. *Science.* 334, 670–4 (2011). [PubMed: 22053049]
59. Chiu JC, Low KH, Pike DH, Yildirim E & Edery I Assaying locomotor activity to study circadian rhythms and sleep parameters in *Drosophila*. *J. Vis. Exp.* 1–8 (2010).
60. Schmid B, Helfrich-Förster C, & Yoshii T A new ImageJ plugin “ActogramJ” for chronobiological analyses. *J Biol Rhythms*, 26, 464–467 (2011). [PubMed: 21921300]
61. Wolf FW, Rodan AR, Tsai LT-Y & Heberlein U High-resolution analysis of ethanol-induced locomotor stimulation in *Drosophila*. *J. Neurosci.* 22, 11035–44 (2002). [PubMed: 12486199]
62. Simon JC & Dickinson MH A new chamber for studying the behavior of *Drosophila*. *PLoS One.* 5, e8793 (2010). [PubMed: 20111707]
63. White KE, Humphrey DM & Hirth F The dopaminergic system in the aging brain of *Drosophila*. *Front. Neurosci.* 4, 1–12 (2010). [PubMed: 20582256]
64. Mendes CS, Bartos I, Akay T, Márka S & Mann RS Quantification of gait parameters in freely walking wild type and sensory deprived *Drosophila melanogaster*. *Elife.* 2, e00231 (2013). [PubMed: 23326642]
65. Shaw PJ, Cirelli C, Greenspan RJ, & Tononi G Correlates of sleep and waking in *Drosophila melanogaster*. *Science.* 287, 1834–1837 (2000). [PubMed: 10710313]
66. Yu Y, et al. Regulation of starvation-induced hyperactivity by insulin and glucagon signaling in adult *Drosophila*. *Elife.* 5, e15693 (2016). [PubMed: 27612383]
67. Qi W, et al. A quantitative feeding assay in adult *Drosophila* reveals rapid modulation of food ingestion by its nutritional value. *Mol. Brain.* 8, 87 (2015). [PubMed: 26692189]
68. Chakrabarti S, Poidevin M, & Lemaitre B The *Drosophila* MAPK p38c regulates oxidative stress and lipid homeostasis in the intestine. *PLoS Genet.* 10, e1004659 (2014). [PubMed: 25254641]

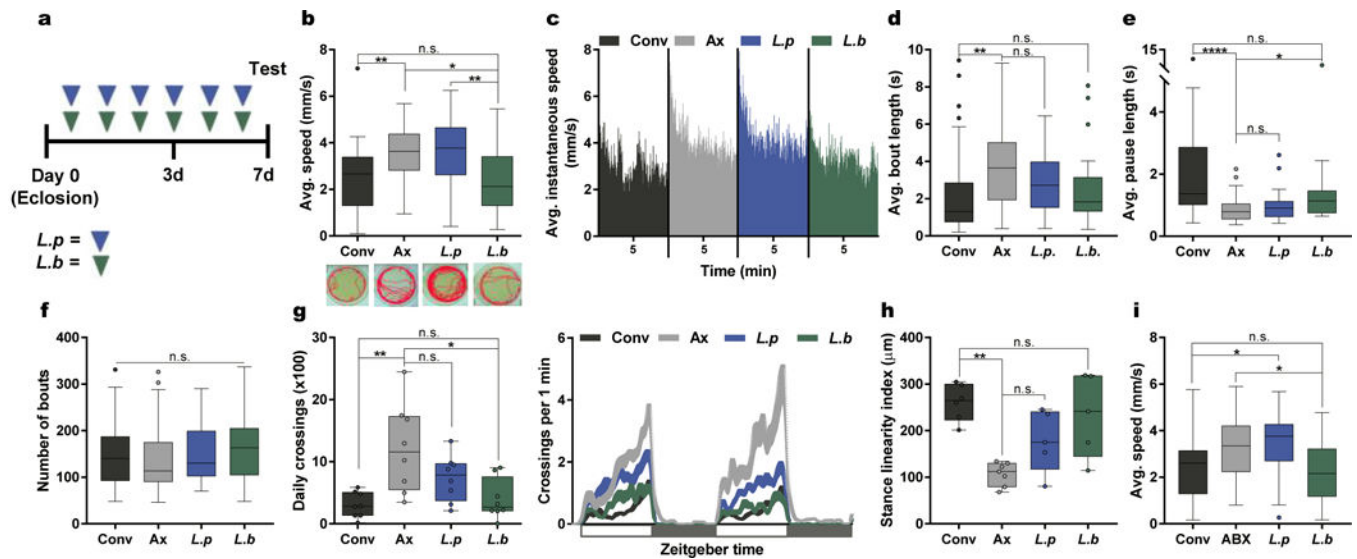


Fig. 1. Select gut bacteria modulate locomotor behavior in flies.

a, Experimental design unless otherwise stated. Briefly, female flies were either left untreated or administered with a bacterial culture or bacterial-derived factors through application to the fly media (40 μ L) daily for 6 days. **b – f**, Analysis of average speed (**b**), average instantaneous speed (**c**), average bout length (**d**), average pause length (**e**), and number of bouts (**f**) of conventional (Conv), axenic (Ax), and *L. plantarum* (*L.p*) or *L. brevis* (*L.b*) mono-associated flies over a 10-min. period. Traces below in (**b**) are representative individuals from each group and dashes below in (**c**) represent the 5-min. mark for each group. (**b**) Conv, $n = 36$; Ax, $n = 36$; *L.p*, $n = 35$; *L.b*, $n = 36$. (**c**) Conv, $n = 23$; Ax, $n = 35$; *L.p*, $n = 23$; *L.b*, $n = 21$. (**d – f**) Conv, $n = 32$; Ax, $n = 36$; *L.p*, $n = 22$; *L.b*, $n = 20$. **g**, Daily activity of virgin female Oregon^R flies over a 2-day light-dark cycle period each lasting 12 hrs., starting at time 0. $n = 8$ /condition. **h**, Stance linearity index calculated for each group. Conv, $n = 6$; Ax, $n = 7$; *L.p*, $n = 5$; *L.b*, $n = 5$. **i**, Average speed of Conv and Conv flies treated with antibiotics (ABX) for 3 days, following which flies were either left naïve or colonized with *L.p* or *L.b*. Conv, $n = 25$; ABX, $n = 29$; *L.p*, $n = 24$; *L.b*, $n = 35$. Box-and-whisker plots show median and interquartile range (IQR). * $P < 0.05$, ** $P < 0.01$, **** $P < 0.0001$. Specific P values are in the Supplementary Material. Kruskal-Wallis and Dunn's post-hoc tests were used for statistical analysis.

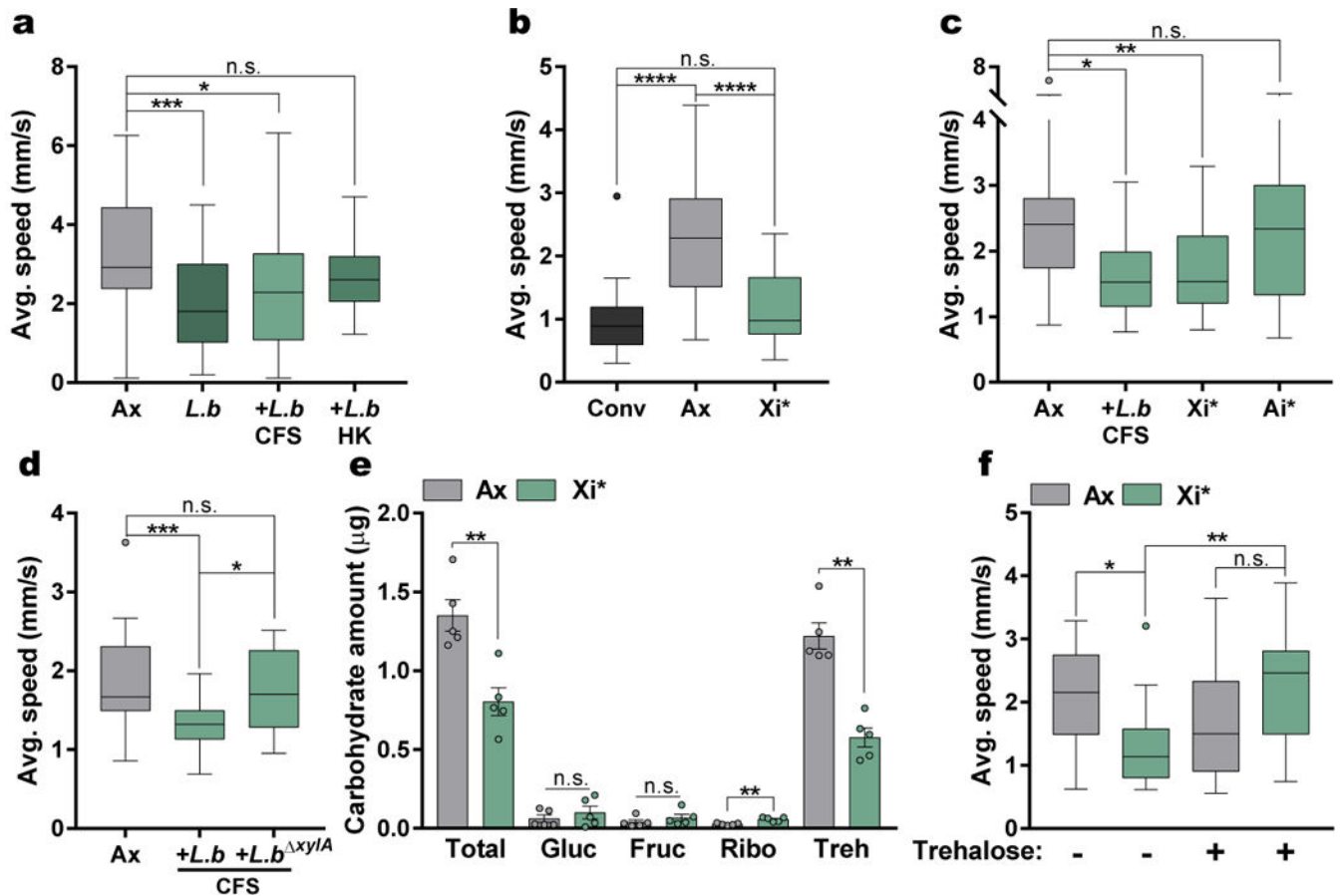


Fig. 2]. Xylose isomerase (Xi) from *L. brevis* alters host locomotion.

a – c, Average speed of Conv, Ax, *L.b* mono-associated, and Ax flies treated with either cell-free supernatant (CFS) from *L.b*, heat-killed (HK) *L.b*, His-tagged xylose isomerase from *L.b* (Xi*, 100 $\mu\text{g}/\text{mL}$), or His-tagged L-arabinose isomerase from *L.b* (Ai*, 100 $\mu\text{g}/\text{mL}$). **(a)** Ax, $n = 57$; *L.b*, $n = 42$; *L.b* CFS, $n = 36$; *L.b* HK, $n = 24$. **(b)** Conv, $n = 17$; Ax, $n = 45$; Xi*, $n = 29$. **(c)** Ax, $n = 31$; *L.b* CFS, $n = 12$; Xi*, $n = 28$; Ai*, $n = 13$. **d,** Average speed of Ax and Ax flies treated with CFS from either WT *L.b* or *xyIA* mutant *L.b* (*L.b xyIA*) bacterial strains. Ax, $n = 28$; *L.b* CFS, $n = 29$; *L.b xyIA* CFS, $n = 18$. **e,** Carbohydrate levels in Ax and Xi*-treated flies. Bars represent mean \pm S.E.M. $n = 5$ samples/condition. **f,** Average speed of Ax flies and Xi*-treated Ax flies either left untreated or supplemented with trehalose (10 mg/mL) for 3 days before testing. Ax, $n = 16$; Xi*, $n = 18$; Ax+Treh, $n = 16$; Xi*+Treh, $n = 17$. Box-and-whisker plots show median and IQR. * $P < 0.05$, ** $P < 0.01$, *** $P < 0.001$, **** $P < 0.0001$. Specific P values are in the Supplementary Material. Kruskal-Wallis and Dunn's (**a – d** and **f**) or Mann-Whitney U (**e**) post-hoc tests were used for statistical analysis. Gluc, glucose; Fruc, fructose; Ribo, ribose; Treh, trehalose.

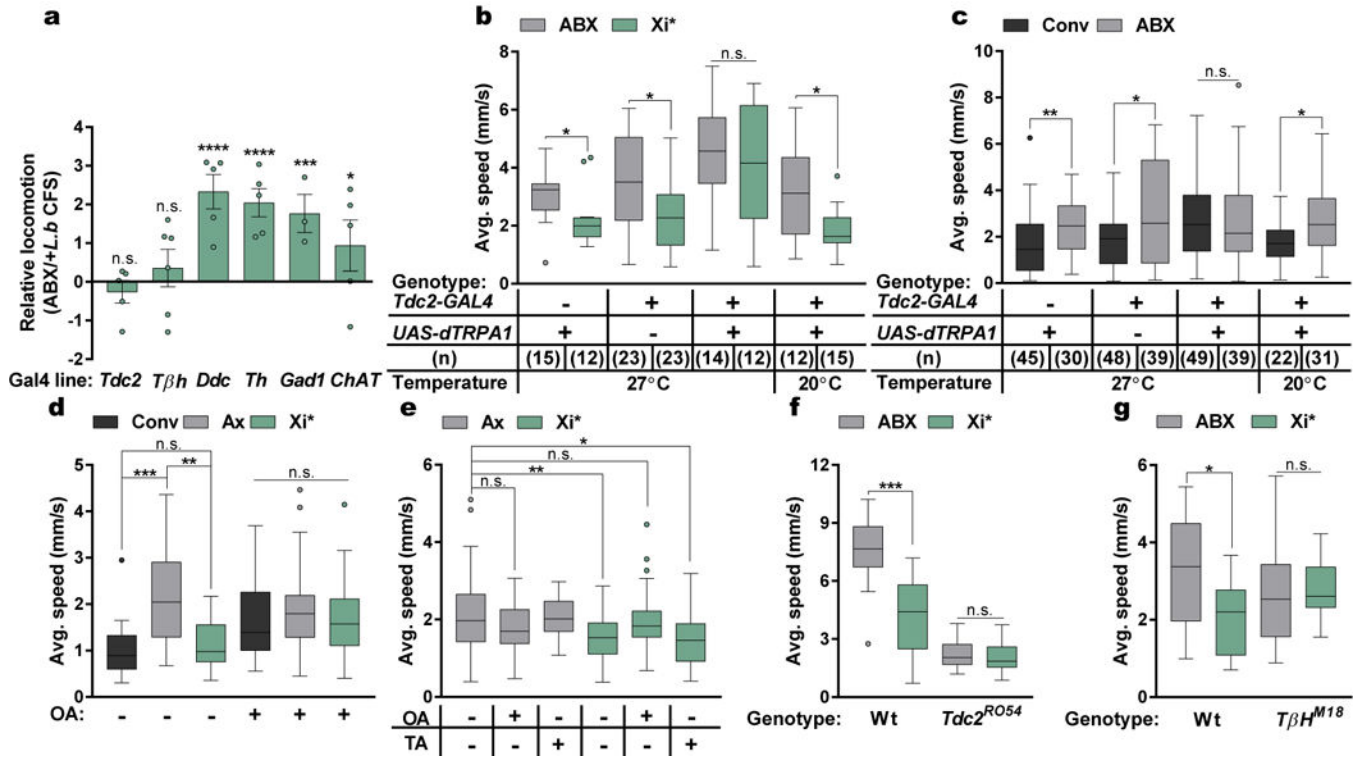


Fig. 3]. Octopamine mediates xylose isomerase-induced changes in locomotion.

a, Difference in average speed for each GAL4 line crossed with *UAS-dTRPA1* at 27°C. Each point denotes an independent trial. Bars represent mean \pm S.E.M. *Tdc2/Ddc/Th/ChAT*, $n = 5$; *Tβh*, $n = 6$; *Gad1*, $n = 3$. **b – c**, Average speed with or without thermogenetic activation. **d – e**, Average speed of flies left untreated or supplemented with octopamine (OA) or tyramine (TA) daily for 3 days. **(d)** Conv, $n = 13$; Ax, $n = 33$; Xi*, $n = 21$; Conv+OA, $n = 29$; Ax+OA, $n = 27$; Xi*+OA, $n = 32$. **(e)** Ax, $n = 58$; Ax+OA, $n = 13$; Ax+TA, $n = 10$; Xi*, $n = 54$; Xi*+OA, $n = 46$; Xi*+TA, $n = 27$. **f – g**, Average speed of antibiotic-treated wild-type (Wt), *Tdc2* null mutants (*Tdc2^{RO54}*), or *Tβh* null mutants (*TβH^{M18}*) left untreated (ABX) or administered with Xi* daily for 3 days. **(f)** Wt (w+): ABX, $n = 12$; Xi*, $n = 17$; *Tdc^{RO54}*: ABX, $n = 19$; Xi*, $n = 17$. **(g)** Wt (Canton-S): $n = 15$; *TβH^{M18}*: ABX, $n = 11$; Xi*, $n = 12$. Box-and-whisker plots show median and IQR. * $P < 0.05$, ** $P < 0.01$, *** $P < 0.001$, **** $P < 0.0001$. Specific P values are in the Supplementary Material. Mann-Whitney U post-hoc tests following a Two-way ANOVA (**a – c**), Kruskal-Wallis and Dunn's post-hoc tests (**d – e**), or Mann-Whitney U post-hoc tests (**f – g**) were used for statistical analysis. *Tdc*, Tyrosine decarboxylase; *Tβh*, Tyramine beta-hydroxylase; *Ddc*, DOPA decarboxylase; *Th*, Tyrosine hydroxylase; *Gad1*, Glutamate decarboxylase 1; *ChAT*, Choline acetyltransferase.